NAVAL POSTGRADUATE SCHOOL
Monterey, California

THESIS

WAVE PROPAGATION OVER COMPLEX BATHYMETRY

by

Timothy Allen Ray

June 2003

Thesis Advisor:	Thomas H.C. Herbers
Second Reader:	Edward B. Thornton

THIS PAGE INTENTIONALLY LEFT BLANK

REPORT DOCUMENTATION PAGE			Form Approved OMB No. 0704-0188
Public reporting burden for this collection of information is estimated to average 1 hour per response, including the time for reviewing instruction, searching existing data sources, gathering and maintaining the data needed, and completing and reviewing the collection of information. Send comments regarding this burden estimate or any other aspect of this collection of information, including suggestions for reducing this burden, to Washington headquarters Services, Directorate for Information Operations and Reports, 1215 Jefferson Davis Highway, Suite 1204, Arlington, VA 22202-4302, and to the Office of Management and Budget, Paperwork Reduction Project (0704-0188) Washington DC 20503.			
1. AGENCY USE ONLY ***(Leave blank)***	**2. REPORT DATE** June 2003	**3. REPORT TYPE AND DATES COVERED** Master's Thesis	
4. TITLE AND SUBTITLE: Wave Propagation Over Complex Bathymetry			**5. FUNDING NUMBERS**
6. AUTHOR(S) Timothy Allen Ray			
7. PERFORMING ORGANIZATION NAME(S) AND ADDRESS(ES) Naval Postgraduate School Monterey, CA 93943-5000			**8. PERFORMING ORGANIZATION REPORT NUMBER**
9. SPONSORING /MONITORING AGENCY NAME(S) AND ADDRESS(ES) N/A			**10. SPONSORING/MONITORING AGENCY REPORT NUMBER**
11. SUPPLEMENTARY NOTES The views expressed in this thesis are those of the author and do not reflect the official policy or position of the Department of Defense or the U.S. Government.			
12a. DISTRIBUTION / AVAILABILITY STATEMENT Approved for public release; distribution is unlimited.			**12b. DISTRIBUTION CODE**

Swell propagates across thousands of kilometers of ocean in almost unchanged parallel wave fronts. Within the nearshore region however, refraction causes wave fronts to turn toward shallow depths transforming the wave field. The Nearshore Canyon Experiment (NCEX) Pilot, conducted from October 10 to October 17, 2002, observed wave transformation across the Scripps and La Jolla canyon system near San Diego, CA. Four Datawell Directional Waverider Buoys, three Nortek Vector PUV recorders, and two pressure sensors were deployed in depths ranging from 10 to 300 m. Observed energy density spectra and mean propagation directions were examined for three case studies representative of the range of observed swell conditions. Observations were compared to predictions of a back-refraction model provided by Dr. William O'Reilly. Observations indicate that refraction causes the waves to propagate along the deep axes of the Scripps and La Jolla canyons. At the shallow canyon heads, the convergence and divergence of ray trajectories cause extreme (2-3 orders of magnitude!) spatial variations in wave energy. Considering the complexity of the canyon environment, predictions of wave transformation agree surprisingly well with observations.

14. SUBJECT TERMS Refraction, Swell Transformation, Scripps Canyon			**15. NUMBER OF PAGES** 54
			16. PRICE CODE
17. SECURITY CLASSIFICATION OF REPORT Unclassified	**18. SECURITY CLASSIFICATION OF THIS PAGE** Unclassified	**19. SECURITY CLASSIFICATION OF ABSTRACT** Unclassified	**20. LIMITATION OF ABSTRACT** UL

NSN 7540-01-280-5500 Standard Form 298 (Rev. 2-89)
Prescribed by ANSI Std. 239-18

THIS PAGE INTENTIONALLY LEFT BLANK

Approved for public release; distribution is unlimited.

WAVE PROPAGATION OVER COMPLEX BATHYMETRY

Timothy Allen Ray
Ensign, United States Naval Reserve
B.S., United States Naval Academy, 2002

Submitted in partial fulfillment of the
requirements for the degree of

MASTER OF SCIENCE IN PHYSICAL OCEANOGRAPHY

from the

NAVAL POSTGRADUATE SCHOOL
June 2003

Author: Timothy Allen Ray

Approved by: Thomas H. C. Herbers
Thesis Advisor

Edward B. Thornton
Second Reader

Mary L. Batteen
Chairman, Department of Oceanography

THIS PAGE INTENTIONALLY LEFT BLANK

ABSTRACT

Swell propagates across thousands of kilometers of ocean in almost unchanged parallel wave fronts. Within the nearshore region however, refraction causes wave fronts to turn toward shallow depths transforming the wave field. The Nearshore Canyon Experiment (NCEX) Pilot, conducted from October 10 to October 17, 2002, observed wave transformation across the Scripps and La Jolla canyon system near San Diego, CA. Four Datawell Directional Waverider Buoys, three Nortek Vector PUV recorders, and two pressure sensors were deployed in depths ranging from 10 to 300 m. Observed energy density spectra and mean propagation directions were examined for three case studies representative of the range of observed swell conditions. Observations were compared to predictions of a back-refraction model provided by Dr. William O'Reilly. Observations indicate that refraction causes the waves to propagate along the deep axes of the Scripps and La Jolla canyons. At the shallow canyon heads, the convergence and divergence of ray trajectories cause extreme (2-3 orders of magnitude!) spatial variations in wave energy. Considering the complexity of the canyon environment, predictions of wave transformation agree surprisingly well with observations.

THIS PAGE INTENTIONALLY LEFT BLANK

TABLE OF CONTENTS

I. INTRODUCTION 1

II. EXPERIMENT AND ANALYSIS 11

III. OBSERVATIONS 17

A. 11 OCTOBER CASE STUDY 17

B. 16 OCTOBER CASE STUDY 23

IV. COMPARISON OF OBSERVED AND PREDICTED SPECTRA 27

A. THE BACK-REFRACTION MODEL 27

B. MODEL-DATA COMPARISONS 28

V. SUMMARY AND CONCLUSIONS 35

VI. LIST OF REFERENCES 37

INITIAL DISTRIBUTION LIST 39

THIS PAGE INTENTIONALLY LEFT BLANK

LIST OF FIGURES

Figure 1. Refraction diagram for 16-second waves from the SSW showing wave crests and rays. Arrowheads on the rays indicate the direction of wave energy propagation. The shoreline, and bottom contours are also shown. (from Munk and Traylor, 1947). 2

Figure 2. Observed versus predicted values in wave height along the beach. Wave heights were observed at beach locations 1 through 12. Predictions are based on refraction diagrams for both 14-second and 12-second period swell from the west-northwest. Maximum wave heights are observed and predicted north of the head of La Jolla Canyon. (from Munk and Traylor, 1947). 4

Figure 3. Nearshore circulation pattern resulting from 12.6 s waves. (from Shepard and Inman, 1950). 5

Figure 4. Azimuthal equidistant projection centered on San Diego, California illustrating windows of possible swell propagation reaching the Southern California Bight from storms around the globe. New Zealand, and Antarctic pack ice significantly limit swell paths from the storm centers in Southern Oceans. (from Munk, Miller, Snodgrass, and Barber, 1963). 7

Figure 5. Schematic map of the Southern California Bight showing three rays for 16.9 s period waves incident to Torrey Pines Beach near Point La Jolla, California. Islands and submerged shoals significantly restrict possible swell paths arriving at Torrey Pines Beach. (from Pawka, et al., 1984). 8

Figure 6. Relative wave heights in the Southern California Bight predicted for October 16th, 2002 (the date of the third case study) by a refraction-diffraction model described by O'Reilly and Guza (1992). (from www.cdip.ucsd.edu). 9

Figure 7. Locations of instruments deployed during the NCEX Pilot experiment within the nearshore environment off Scripps Beach. The site features two submarine canyons, the larger La Jolla Canyon along a NNW to SSE axis, branching into the narrow Scripps Canyon to the east. 12

Figure 8. Pressure (P) sensor used in the NCEX Pilot Experiment. The p-sensor is mounted in a red fiberglass tripod equipped with lead feet to ensure stability on the ocean bed. 13

Figure 9. The Nortek pressure and horizontal velocity recorder (PUV) ready to be deployed during the NCEX Pilot Experiment. 14

Figure 10. Location of NCEX and permanently maintained directional waverider buoys. (from www.cdip.ucsd.edu) 15

Figure 11. Observed energy density spectra and mean directions (as a function of frequency) north of Scripps Canyon on October 11th. The dashed lines indicate the incident wave conditions measured well offshore in deep water at the Outer Torrey Pines Buoy, buoy 100. Observations of wave conditions north of Scripps Canyon are indicated in color. Note the dramatic variations in wave conditions at swell (<0.1 Hz) frequencies. 19
Figure 12. Observed energy density spectra and mean directions surrounding Scripps Canyon on October 11th. (same format as Figure 11) 20
Figure 13. Observed energy density spectra and mean directions in the southern region of the canyon system on October 11th. P-sensor records do not contain directional information. Extreme refraction is evident in the observed turning of the mean direction at the swell peak by about 110º from 210º at buoy 100 to 320º at PUV1. (same format as Figure 11) 21
Figure 14. A refraction diagram for 16 second swell incident from the SSW -- conditions similar to those observed during the NCEX Pilot Experiment. (from Munk and Traylor, 1947) 22
Figure 15. Energy and directional spectra at locations north of Scripps Canyon during the October 16th case study. (same format as Figure 11) 24
Figure 16. Energy and directional spectra at locations surrounding Scripps Canyon during the October 16th case study. (same format as Figure 11) 25
Figure 17. Energy and directional spectra at locations between Scripps Canyon and La Jolla Canyon, and south of La Jolla Canyon during the October 16th case study. (same format as Figure 11).....26
Figure 18 Observed (solid) and predicted (dashed) energy spectra and mean direction as a function of frequency on October 11. Buoy 100 provided the incident wave spectra for the back-refraction model calculation. Instrument locations are indicated with color: Buoy 100 - black, buoy 113 - red, buoy 114 - purple, buoy 115 - blue, and buoy 116 - green. 29
Figure 19. Observed (solid) and predicted (dashed) spectra on October 16. Buoy 100 provided the incident spectra for the back-refraction model calculation. Instrument locations are indicated with color: Buoy 100 - black, buoy 113 - red, buoy 114 - purple, buoy 115 - blue, and buoy 116 - green. 31
Figure 20. The spectra observed by buoy 100 and buoy 115, along with the modeled spectra at three locations: at buoy 115, 60 m north of buoy 115, and 60 m west of buoy 115. The modeled spectra 60 m north, and 60 m west of buoy 115 are in better agreement with the observed spectrum at buoy 115. ...32
Figure 21. GPS tracked locations for buoy 115 over the course of the experiment. Although modeled spectra at locations 60 m west and north of the buoy (away from the canyon wall) were closer to observations made by buoy 115, the buoy drifted primarily to the southeast (into the canyon). 33
Figure 22. Observed and predicted significant wave height on October 11. Red and blue numbers correspond respectively to observed and predicted significant wave height. The incident significant wave height observed at buoy 100 was 0.38 m. Model predictions for PUV1 were not available, thus only the observed wave height is shown.

THIS PAGE INTENTIONALLY LEFT BLANK

ACKNOWLEDGMENTS

Like many people, I have always enjoyed watching ocean waves break at the coast, and thus I am sincerely thankful for opportunity to study nearshore waves. My research has given me a new appreciation for the incredible complexities of one of natures most beautiful processes.

My advisor, Professor Thomas Herbers, deserves the utmost thanks for his patience, guidance, enthusiasm, and support. Dr. Herbers graciously allowed me to join his laboratory and we began working immediately. Within days I found myself onboard the R/V GORDON SPROUL deploying sensors for the NCEX Pilot Experiment. Dr. Herbers is an excellent example of a professor dedicated not only to science, but to students.

I cannot thank Mr. Paul Jessen enough for his extensive support at every stage of this study. His expertise in oceanographic sensors, data processing, and programming made this thesis possible. In addition, Mr. Jessen brightened several spring and summer mornings with visits from his infant daughter Genevieve, a young oceanographer-in-training.

Dr. William O'Reilly deserves great thanks for graciously sharing his modeled back-refraction predictions. His enthusiasm for waves is contagious, and his patient and clear explanations of wave transformations greatly aided my understanding of the research.

Additionally, I'd like to thank Professor Edward Thornton for kindly accepting to be my second reader; and Dr. Steve Elgar for coordinating the NCEX Experiment and providing the high-resolution bathymetry for this study.

Most importantly, I thank my family for their enduring love and support.

THIS PAGE INTENTIONALLY LEFT BLANK

I. INTRODUCTION

The nearshore environment is crucial to modern naval operations. The need for environmental information at a tactical level has increased as naval power projection continues to focus on the littoral environment. Amphibious landings, nearshore reconnaissance, and SEAL team insertion are only cursory examples of naval operations dependent on accurate nowcasts and forecasts of the nearshore environment. Understanding the transformation of swell over complex coastal bathymetry; and the resulting variations in wave heights, associated sediment transport, and surf zone circulation is critical to the modern warfighter.

Waves travel over thousands of kilometers largely unchanged across ocean basins. Only a few kilometers from the coast, swell reach shallow water and can be dramatically transformed by bottom topography, typically by processes such as refraction, diffraction, and reflection. Refraction, the turning of wave trains caused by the dependence of wave speed on water depth, can be modeled precisely when high resolution bathymetry and boundary conditions are available. Diffraction and reflection, which cause dispersion of wave energy away from regions of discontinuities, are complex processes that are more difficult to model accurately for realistic coastal settings.

The nearshore environment off Scripps Beach, near San Diego, California provides an excellent location to study the transformation of ocean swell. The relatively straight coastline extends along a NNW and SSE axis from the Scripps Institution of Oceanography to the La Jolla Beach and Tennis Club where the shoreline curves sharply to the WNW toward Pt. La Jolla for approximately 1000 meters (Figure 1). The straight coastline is deceiving, hiding complex undersea topography that causes extreme wave height variations over distances less than 100 m. The environment is dominated by the dramatic depth changes of two deep undersea canyons that extend to within 250 meters of the shoreline (Figure 1). The walls of the larger and wider La Jolla

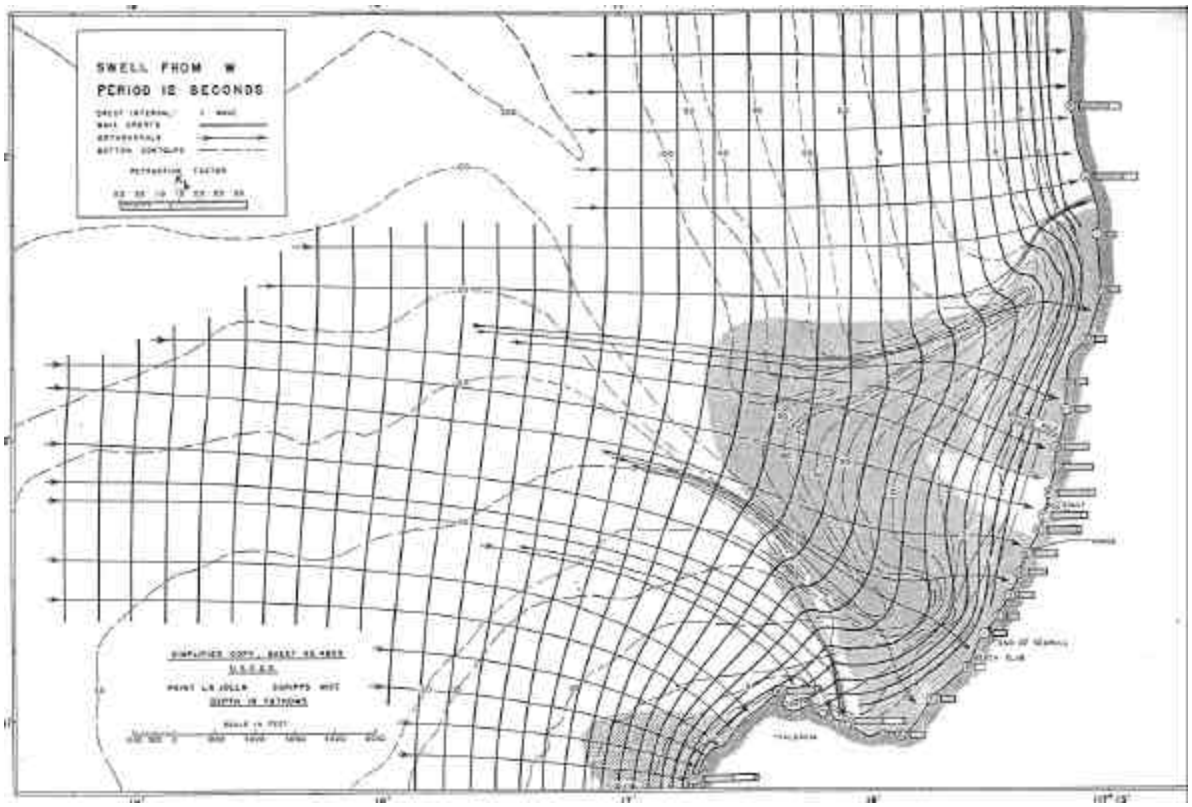

Figure 1. Refraction diagram for 16-second waves from the SSW showing wave crests and rays. Arrowheads on the rays indicate the direction of wave energy propagation. The shoreline, and bottom contours are also shown. (from Munk and Traylor, 1947).

canyon have slopes as large as 1:1, but even more dramatic is the narrow Scripps canyon, a northern branch of La Jolla Canyon. The walls of Scripps canyon have been measured to have a slope as steep as 7:1. Both rocky canyons are covered with a thin layer of sand and silt, with rocky points at the southern end of the canyon rims.

Munk and Traylor (1947) conducted the first qualitative study of the effects of bottom topography on wave energy transformation over the Scripps Canyon. Refraction was reviewed in light of other processes affecting the transformation of shallow water waves. As waves approach the coastline, they begin to feel the bottom when the water depth is less than one half the wavelength. Closer to the coast, when waves enter shallow water, their wave speed equals $\sqrt{gh}$ where g is the acceleration of gravity and h is the water depth. Hence, waves slow down as the depth decreases. Where bottom topography is irregular, some parts of the wave crest will feel the bottom before others. Thus, as a wave crest approaches the shore, the portion of the wave crest entering shallow

water slows down, causing the wave crest to swing around toward areas of shallow water. If the bottom slope is sufficiently gentle, the wave crests tend to conform to the bottom topography and arrive at the coastline at near normal incidence. Snell's Law describes this effect: the ratio $\sin(q)/c$, is conserved where q is the angle of approach and c is the wave phase velocity. In areas with complex bottom topography, wave refraction diagrams, such as Figure 1, are useful to visualize changes in wave direction and height.

In the refraction diagram, wave crests are shown as lines usually parallel to shore, while the direction of wave propagation is shown as a series of rays that are orthogonal to wave crests. In regions where rays converge, wave energy (and height) increases, and in areas where ray traces diverge, wave energy decreases. The example refraction diagram, Figure 1, illustrates the dramatic transformation of wave crests that are initially straight in deep water. The arrows on ray trajectories indicate the propagation paths of incoming waves. The change in spacing between rays indicates convergence and divergence zones, which in Figure 1 are also signified by shading and crosshatching. Notable features include a large area of divergence and reduced wave heights to the south of Scripps canyon, extending to the northeastern side of Pt. La Jolla. Convergence along the north rim of Scripps Canyon causes large waves at Black's Beach on the north side of the Scripps Canyon, and convergence along the Southern rim of La Jolla Canyon causes focusing at Pt. La Jolla.

The wave period of ocean swell affects the degree of wave refraction. Waves with longer periods "feel" the ocean bottom in deeper water. Longer period swell (e.g., 12 and 14 seconds in Figures 1 and 2, respectively) are strongly affected by the canyons at Scripps Beach, whereas shorter period wind waves do not feel the bottom until they have passed over the canyon onto the relatively uniform beach, and are thus less affected by refraction at this site.

Munk and Traylor (1947) compared their theoretical wave refraction estimates with visual observations of wave heights collected by shore-based observers (Figure 2). Although inaccuracies of visual observations, the difficulty of producing high resolution refraction diagrams, and the exclusion of the effects of diffraction or reflection

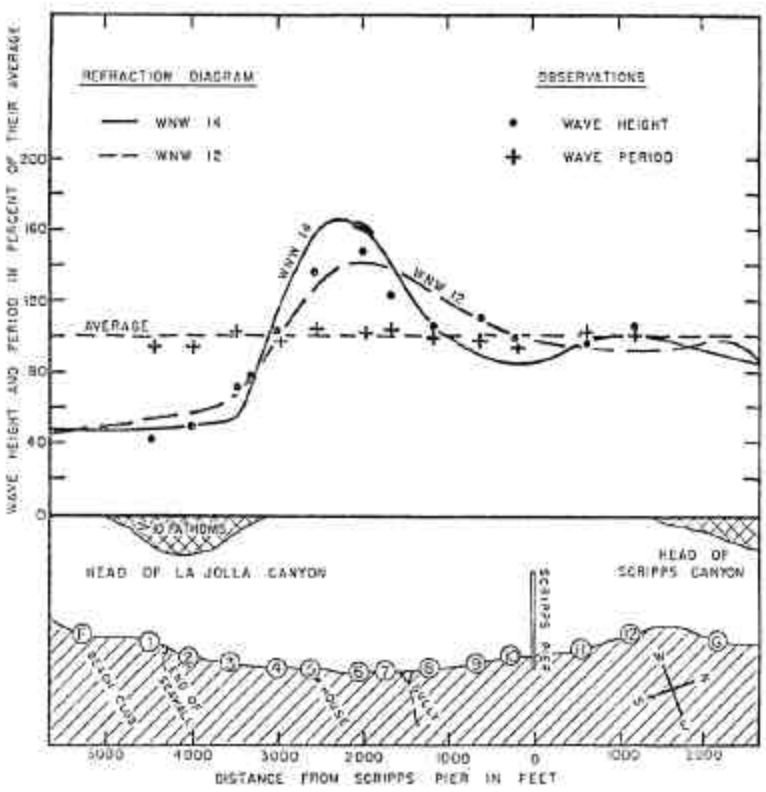

Figure 2. Observed versus predicted values in wave height along the beach. Wave heights were observed at beach locations 1 through 12. Predictions are based on refraction diagrams for both 14-second and 12-second period swell from the west-northwest. Maximum wave heights are observed and predicted north of the head of La Jolla Canyon. (from Munk and Traylor, 1947).

introduced considerable uncertainty in these comparisons, the observed and predicted wave heights generally agree to within about 10%. As illustrated in Figure 2, refraction causes a redistribution of 14 second swell wave energy at the surf zone with variations as high as 300% over only 300 meters of coastline. Actual variations may be even higher in the vicinity of the canyon heads where wave height gradients in refraction model results may have been smoothed out by low resolution bathymetry and where observations were not available.

The effects of swell refraction extend beyond the variation of wave height at the coast. As wave energy is redistributed by bathymetry, variations in wave set-up at the shoreline cause horizontal circulation cells, which in turn affect sediment transport

patterns. Shepard and Inman (1950) studied the effects of wave refraction on nearshore water circulation.

Observations using dye, drifting tri-floats, and neutrally buoyant floats suggest that the fundamental structure of nearshore circulation results from irregularities in the bottom topography. The observed nearshore circulation cells can be explained qualitatively in response to areas of convergent and divergent wave energy (Figure 3).

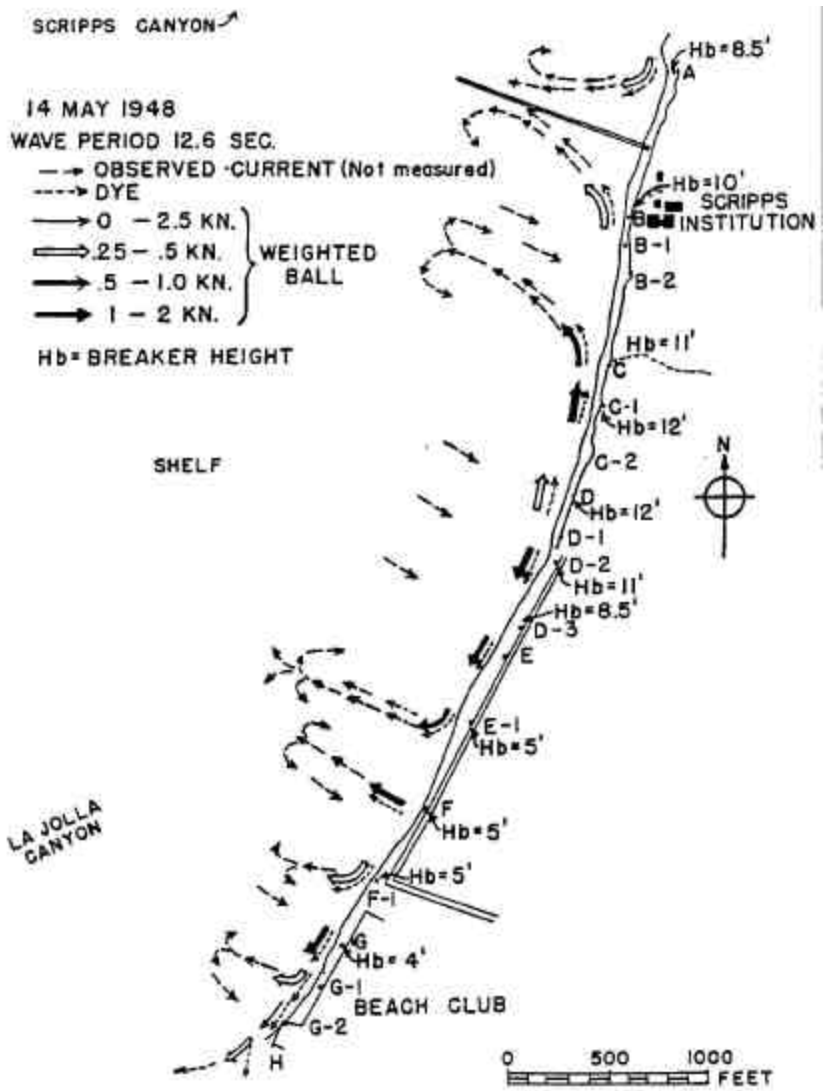

Figure 3. Nearshore circulation pattern resulting from 12.6 s waves. (from Shepard and Inman, 1950).

A major component of nearshore circulation cells are rip currents. Rip currents develop where water flowing alongshore away from convergence zones meets water flowing from divergent zones. The combined water mass then flows seaward until it is deflected by larger longshore coastal currents. Fundamentally, nearshore circulation cells depend on the refractive effects of bottom topography.

Swell observed on California beaches are the results of storm events occurring around the globe. In the classic experiment, *Propagation of Ocean Swell Across the Pacific*, Snodgrass et al. (1966) studied the evolution of swell from its generation in storm events in the South Pacific, through its propagation across the Pacific Ocean, to the dissipation of wave energy on distant shores. Analysis of their observations showed surprisingly little wave energy is dissipated in the open ocean, even after swells have traveled distances greater than 12000 nautical miles. Figure 4 shows possible wave paths that reach Southern California from storm events in the Southern Hemisphere and the Gulf of Alaska. In the Northern Hemisphere, waves arriving at Southern Californian beaches from directions north of 295º are blocked by Point Conception; and waves originating from locations east of 150º are blocked by Point Eugenia, Baja California, Mexico. (Munk and collaborators, 1963) Observations often reveal simultaneous swell arrivals from different propagation windows.

The Southern California Bight, through which swell must traverse on its path to Pt. La Jolla, contains many offshore islands, shallow submerged banks, canyons, and other complicated coastal bathymetry, and extends from 32ºN South of San Diego to 34.5ºN at Point Conception. Although islands shadow wave energy in their lee (Figure 5), and refractive and diffractive effects decrease wave energy, little discernable cross swell is seen in the lee of islands on the spatial scale of the Southern California Bight. (Emery, 1958). Wave heights, however, do vary at different locations of the Southern California Bight as a result of both the blocking effects of islands and the scattering effects of submerged shoals. Whereas refraction affects primarily longer period waves, island blocking affects all wave periods. Pawka et al. (1984) compared observations of wave height to model results simulating the effects of island blocking and wave refraction at several locations across the Southern California Bight.

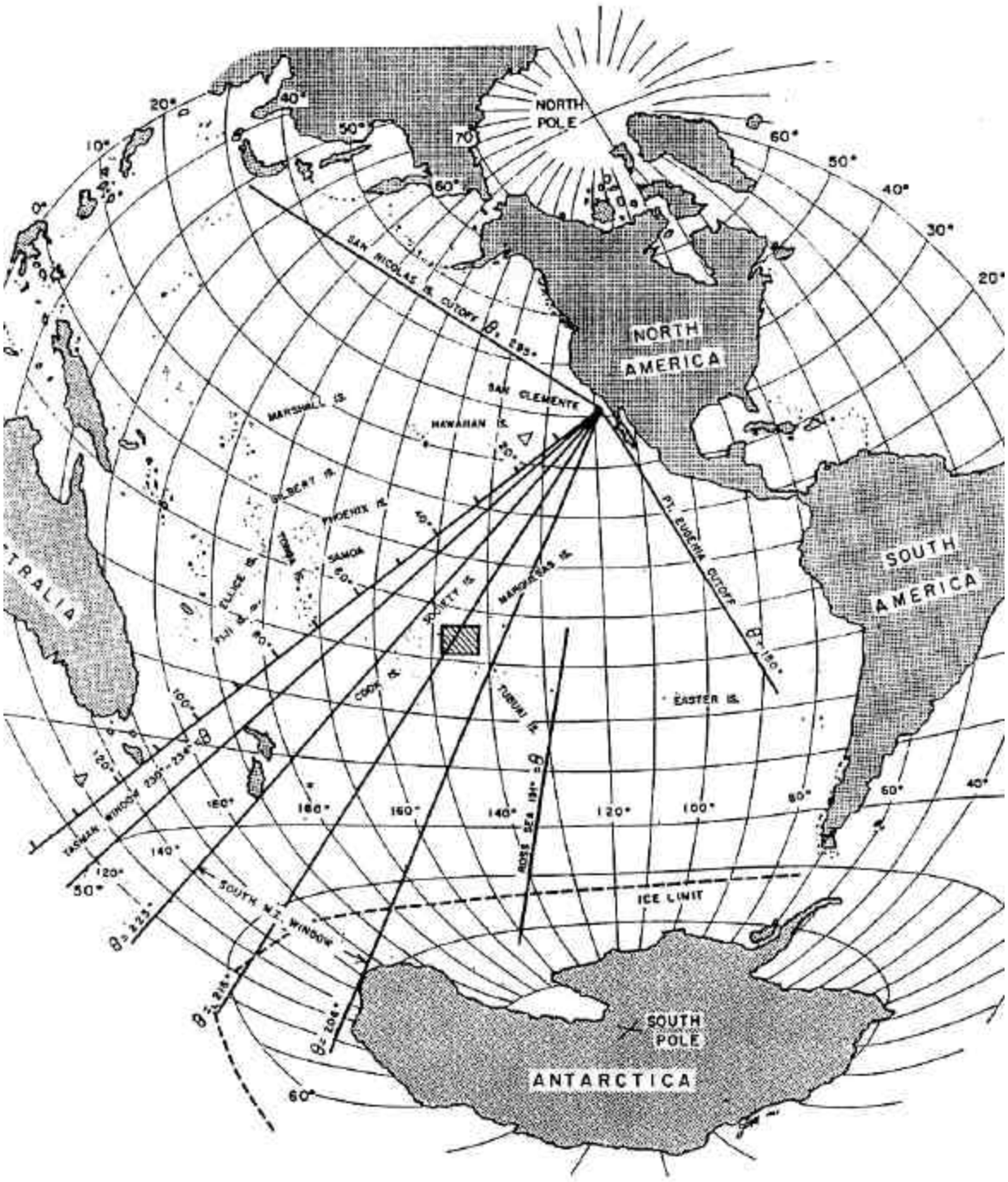

Figure 4. Azimuthal equidistant projection centered on San Diego, California illustrating windows of possible swell propagation reaching the Southern California Bight from storms around the globe. New Zealand, and Antarctic pack ice significantly limit swell paths from the storm centers in Southern Oceans. (from Munk et al., 1963).

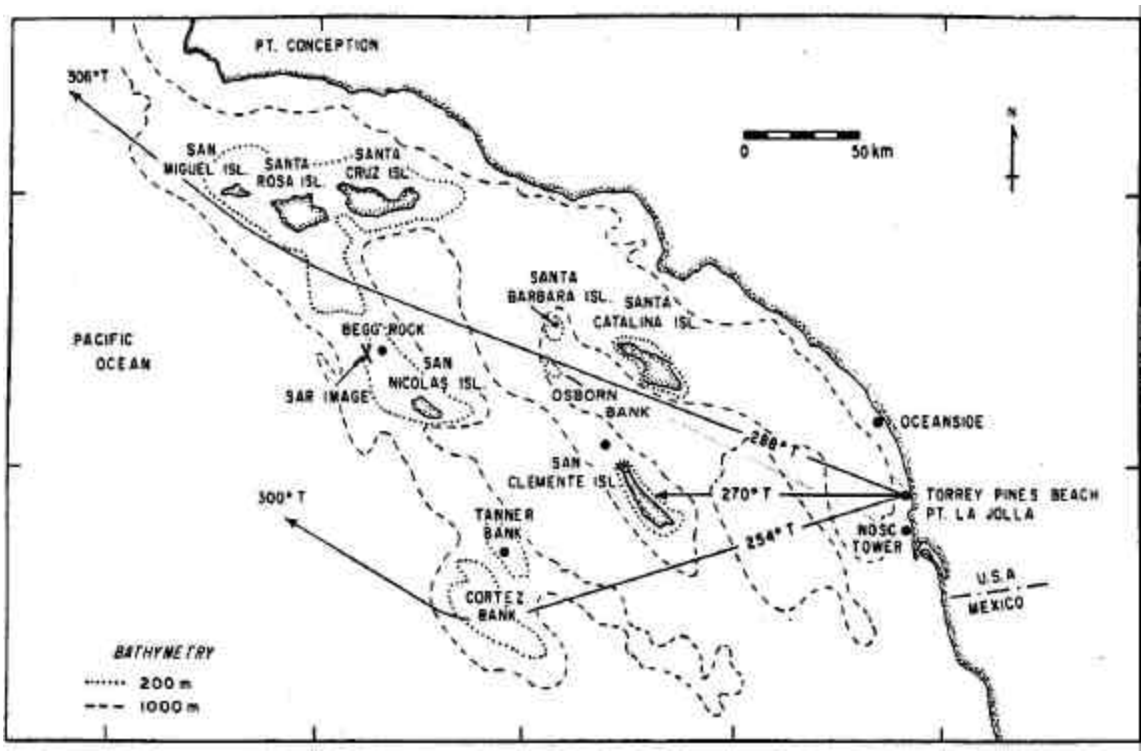

Figure 5. Schematic map of the Southern California Bight showing three rays for 16.9 s period waves incident to Torrey Pines Beach near Point La Jolla, California. Islands and submerged shoals significantly restrict possible swell paths arriving at Torrey Pines Beach. (from Pawka, et al. , 1984).

The model used by Pawka et al. is a continuous spectrum refraction model based on the conservation of wave energy and wave frequency along a ray. The model requires a linear wave field without energy sources or sinks, and a slow variation of bathymetry and wave amplitude. The refraction model employs a continuous spectrum to avoid caustic zones, and back-refracts wave rays into deep water spectra. Rays intercepting islands are terminated.

The entire swell spectrum is affected by offshore islands, sand banks, and headlands (Figure 6). Additionally diffraction effects can be important for directionally narrow wave fields in the vicinity of complex bathymetry. O'Reilly and Guza (1992) compared wave energy predictions from refraction and refraction-diffraction models at Mission Beach, near San Diego, California. Although the refraction model is inaccurate when the incident wave spectrum is narrow, or when the near-field bathymetry is complex, in practical applications with reasonably broad spectra and mild bathymetry the

refraction model agrees well with the refraction-diffraction model. In the case of extremely broad directional incident spectra, the refraction-diffraction model produces significant errors due to the small angle approximation inherent in the model. Limitations of both models in complex (e.g. the Scripps Canyon) environments where both diffraction and large propagation angles are expected are not well understood.

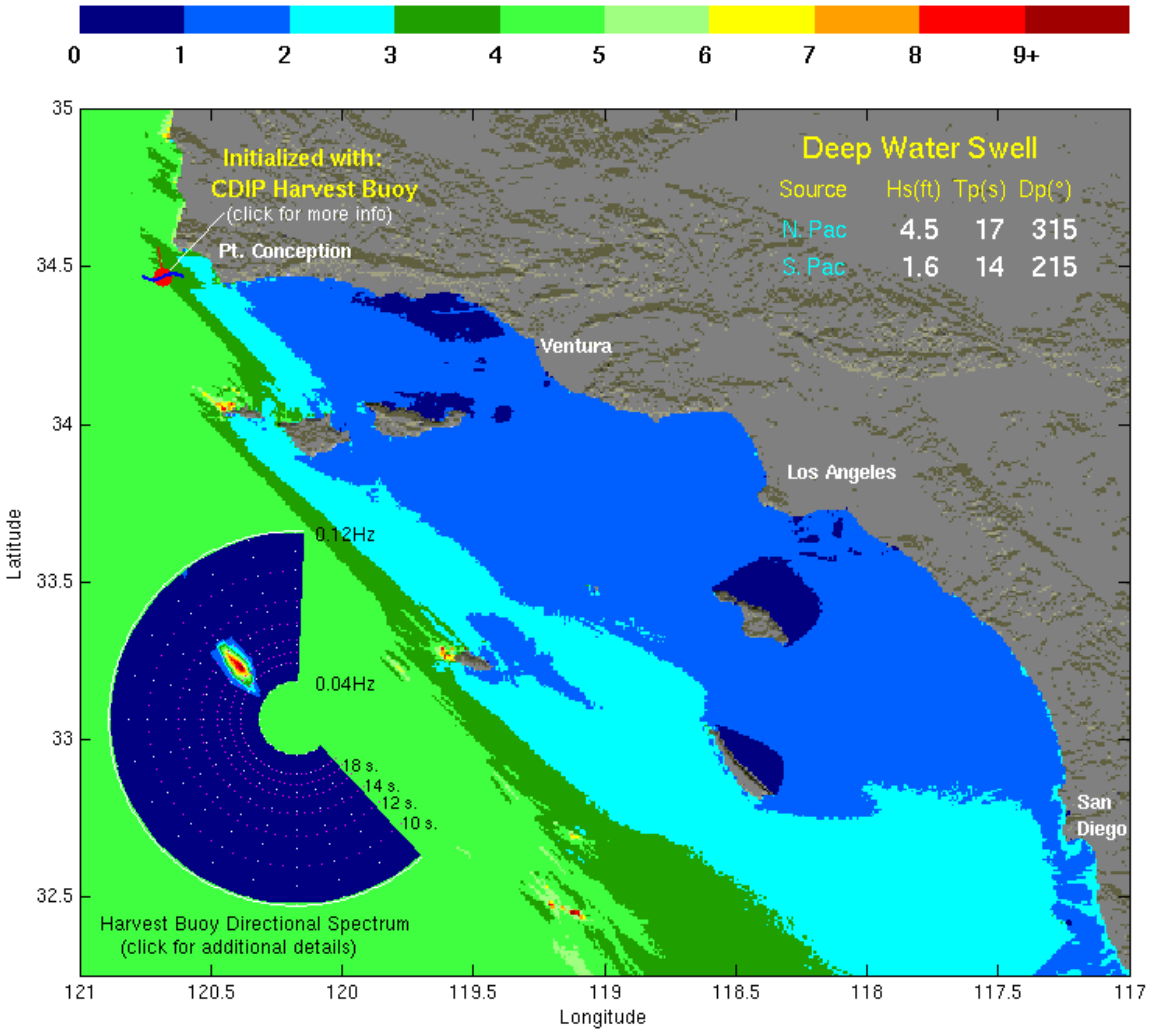

Figure 6. Relative wave heights in the Southern California Bight predicted for October 16th, 2002 (the date of the third case study) by a refraction-diffraction model described by O'Reilly and Guza (1992). (from www.cdip.ucsd.edu).

THIS PAGE INTENTIONALLY LEFT BLANK

II. EXPERIMENT AND ANALYSIS

Munk and Traylor's 1947 pioneering study of wave refraction at Scripps Beach was primarily qualitative owing to limitations of visual observations and manual ray computations. Fifty-five years later, computer systems, and advanced instrumentation allow the collection and processing of large datasets, and accurate modeling of wave transformation over the nearshore canyons. For 8 days, from October 10, 2002 through October 17, 2002, data were recorded by two pressure (P) sensors, three Nortek Vector (PUV) sensors recording pressure and horizontal velocity, and four Datawell Directional Waverider buoys measuring wave height and direction. These instruments were deployed in areas around the Scripps Canyon (Figure 7) as part of a pilot study in preparation for the Nearshore Canyon Experiment (NCEX) scheduled for the fall of 2003.

As shown in Figure 7, most instruments were deployed in the region around Scripps Canyon, with sparser coverage across the entire nearshore region. Refraction model computations were used to select sensor locations in places where the most extreme wave energy transformation is expected. These extreme transformations are projected to occur primarily on the north side and at the head of Scripps Canyon where the waverider buoys (113-116), one pressure sensor (P2) and one PUV sensor (PUV3) are located. The remaining sensors (P1, PUV1, PUV2) were deployed between the canyons and on the south side of La Jolla Canyon to quantify wave transformation over the entire canyon region.

After a series of bathymetry survey sweeps in the vicinity of target pressure sensor locations verified acceptable water depths and bottom slopes; two pressure sensors, designated P1 and P2, were deployed on the shelf between Scripps and La Jolla Canyons (Figure 7). The pressure sensors were fitted in fiberglass bottom tripods with acoustic releases for easy recovery (Figure 8). All sensors were deployed from the R/V GORDON SPROUL using differential GPS and targeting software for precise positioning to within about 5 meters of the desired locations.

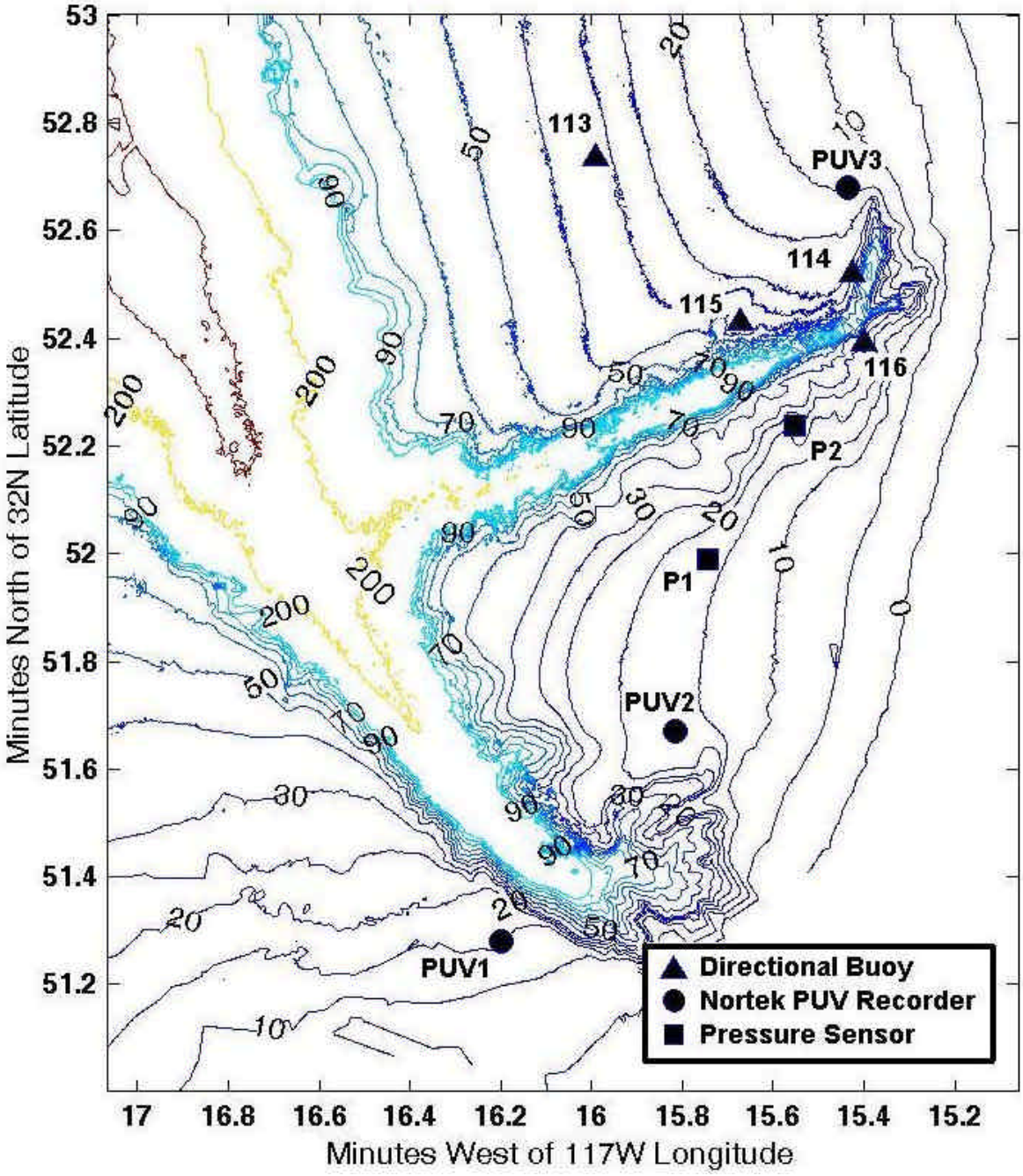

Figure 7. Locations of instruments deployed during the NCEX Pilot experiment within the nearshore environment off Scripps Beach. The site features two submarine canyons, the larger La Jolla Canyon along a NNW to SSE axis, branching into the narrow Scripps Canyon to the east.

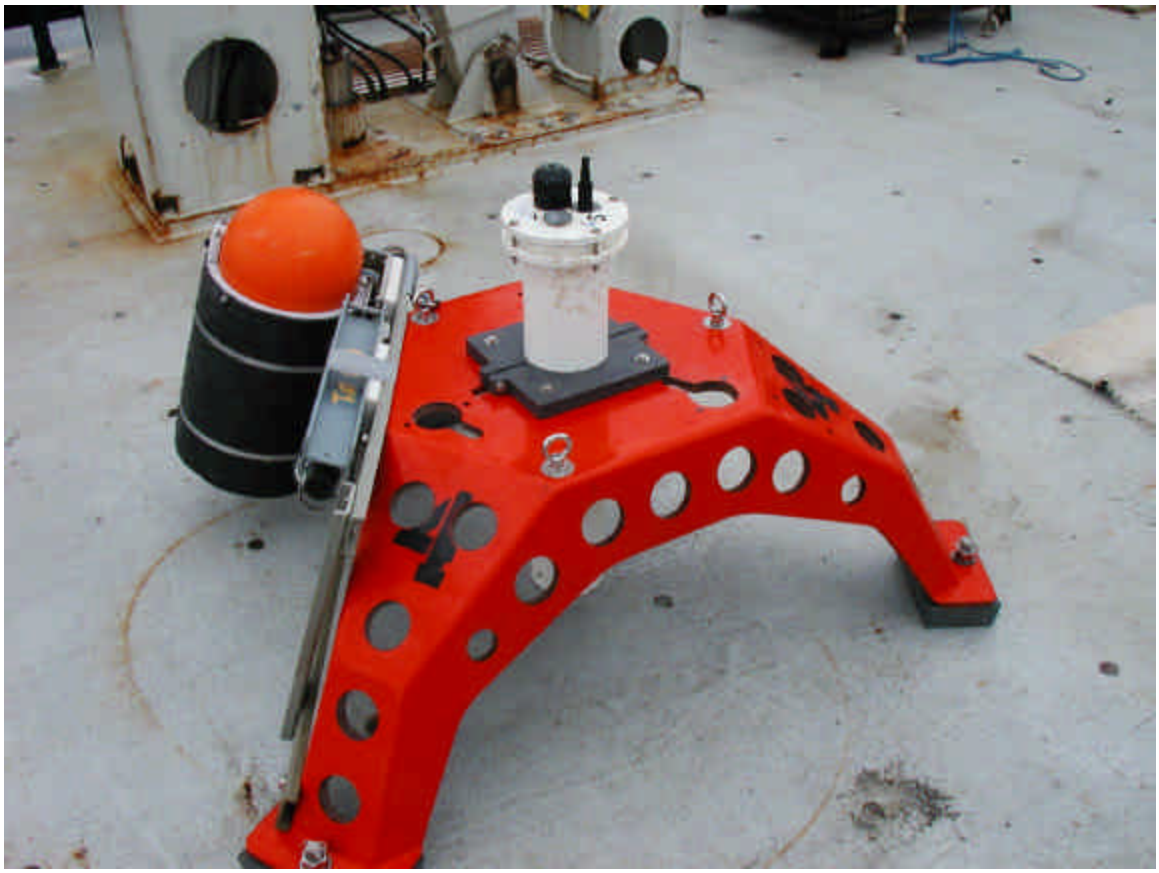

Figure 8. Pressure (P) sensor used in the NCEX Pilot Experiment. The p-sensor is mounted in a red fiberglass tripod equipped with lead feet to ensure stability on the ocean bed.

Divers from the Scripps Institution of Oceanography measured the heights of the instruments above the sea bed, a measurement needed to accurately determine the attenuation of pressure over the water column. Pressure records sampled at 1 Hz were recorded internally in the instruments. Recorded data were downloaded upon sensor recovery.

Following the pressure sensor deployment, and after further bathymetry surveys, the three Nortek Vector PUV sensors were deployed (Figure 9). PUV1 was deployed southwest of the head of La Jolla Canyon, PUV2 was deployed on the shelf between the canyons, and PUV3 was deployed near the head of Scripps Canyon. Similar to the pressure sensor moorings, the PUV sensors were mounted in fiberglass tripods to which a polypropylene line and a surface float were attached for recovery operations.

Figure 9. The Nortek pressure and horizontal velocity recorder (PUV) ready to be deployed during the NCEX Pilot Experiment.

The Nortek Vector PUV sensors contain a pressure sensor and a three-component acoustic Doppler velocimeter. The combined pressure (p) and horizontal velocity (u,v) data provide height and directional wave data equivalent to measurements of a pitch and roll buoy. The pressure and velocity time series were recorded internally with a sample frequency of 2 Hz.

Waverider buoys 113 through 116 were deployed in advance of the experiment and continue to operate. These buoys and several other permanent directional waverider buoys in the region are maintained through the University of California at San Diego's Coastal Data Information Program (CDIP). The permanent Outer Torrey Pines buoy designated Buoy 100, located approximately 6.7 miles west of Torrey Pines State Beach (Figure 10) provided measurements of incident wave energy and direction spectra in deep water.

The Datawell Directional Waverider buoys measure acceleration in three directions and the tilt of the buoy from which the x, y, and z displacements are evaluated in a fixed reference frame. These buoys sample at 1.28 Hz, and time series are processed internally to produce wave height spectra and directional moments. The buoy data are transmitted to receivers onshore via an HF radio link. The buoy is moored with an elastic line so that wave motions at swell and wind sea frequencies (nominally 0.04 - 0.5 Hz) are measured with negligible distortion.

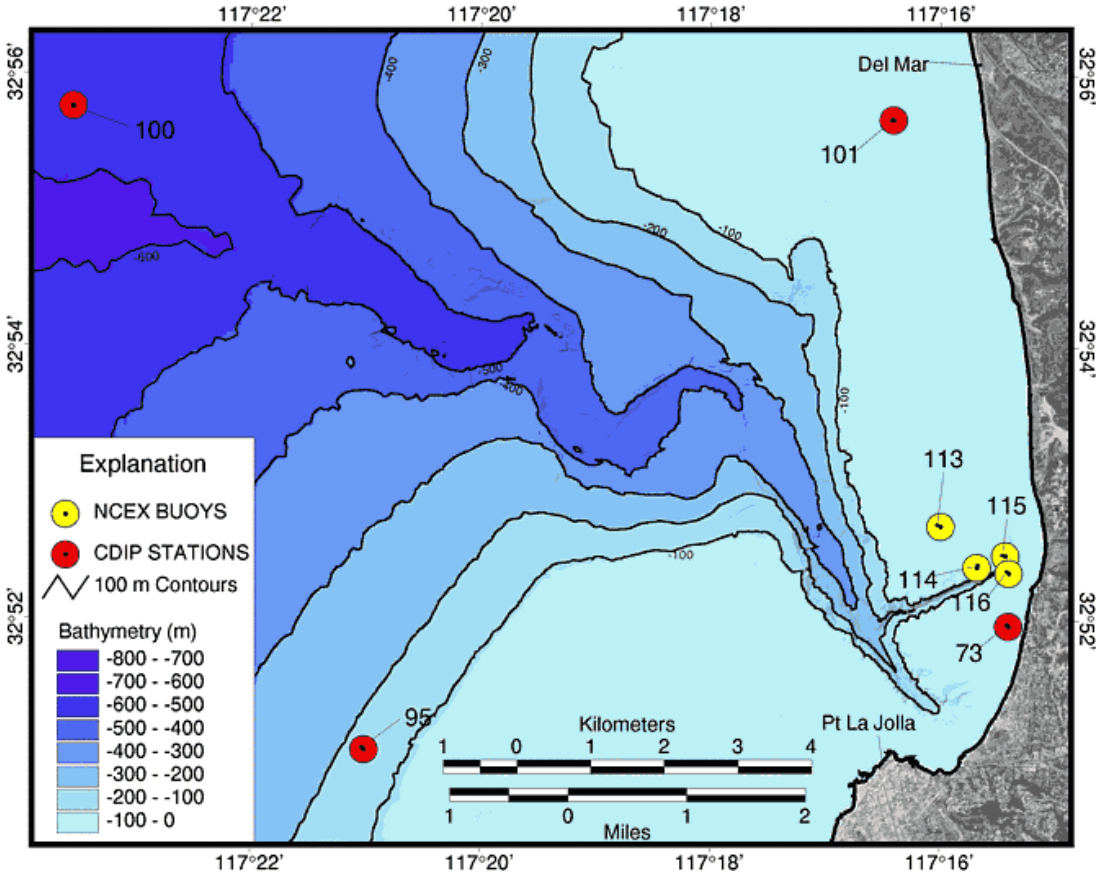

Figure 10. Location of NCEX and permanently maintained directional waverider buoys. (from www.cdip.ucsd.edu)

The pressure and horizontal velocity signals collected by the P and PUV-sensors attenuate with depth. Surface height spectra were estimated from the measured pressure spectra by applying a correction in the frequency domain for the hydrodynamic attenuation of waves over the water column, based upon linear wave theory.

Whereas P1 and P2 provide only surface height spectra, additional directional information is available from each PUV dataset. Estimates of a mean wave direction at each frequency were calculated using a standard technique based upon pressure-velocity cross-spectra (e.g. Herbers et al. 1999) Unfortunately PUV2 did not record meaningful data throughout most of the experiment, and measurements collected by this instrument are not included in this analysis.

Processed observations of the Datawell Directional Waverider buoys were provided by Dr. William O'Reilly of the Scripps Institution of Oceanography. Wave height spectra were obtained directly from the vertical displacement measurements whereas the mean direction estimates at each frequency are based on cross-spectra between vertical and horizontal displacements. All estimates of wave spectra and mean directions presented below are based on 3 hour-long data records.

III. OBSERVATIONS

Observations made during the NCEX Pilot were compared in three sub-regions within the nearshore environment surrounding Scripps Canyon. These sub-regions were selected to simplify spectral comparison while facilitating the examination of wave transformation across different paths of the canyon system. The first sub-region, north of Scripps Canyon includes the Waverider Buoys 113, 114, and 115, and PUV3. The second sub-region, surrounding the head of Scripps Canyon includes buoys 115, 116, PUV3 and P2, and the third sub-region, between Scripps and La Jolla Canyon, and south of La Jolla Canyon, includes both pressure sensors, PUV1 and PUV2. Wave height and directional spectra measured at the offshore buoy 100 are included in each sub-regional comparison to characterize the "undisturbed" incident wave field seaward of the canyons and shelf.

Three representative 3-hour time intervals spanning the range of incident swell conditions observed over the duration of the experiment were selected as case studies: 11 October 2002 from 1800 to 2100 (PDT), 14 October 2002 from 0300 to 0600 (PDT), and 16 October 2002 from 1500 to 1800 (PDT). These case studies will be referred to by the date observations were made. Comparisons of energy and directional spectra are restricted to the frequency range 0.05 - 0.30 Hz, containing the dominant swell and wind seas.

The incident wave field on October 14 was very similar to that of October 11, and therefore this case is not discussed here. On October 16, however, a significant shift in the incident wave direction had occurred in the swell band, and dramatic changes in wave transformations were observed.

A. 11 OCTOBER CASE STUDY

The incident wave conditions observed at buoy 100 (Figure 11) show the dominant swell with a wave period of about 15 seconds arriving from 209º to 214º True North. This swell peak contains almost one order of magnitude more energy than a secondary peak observed at about 10.5 seconds, incoming from 227º. Higher frequency

local wind driven waves are seen with periods less than 5 seconds, a peak energy at 4 seconds and a general propagation direction of 270º. The observed energy spectra and mean directions as a function of frequency are compared for each sub-region in Figures 11 - 13.

Swell frequencies experience significant evolution across the canyons. At the 15 second swell peak, energy levels are amplified (relative to the offshore buoy 100) at both PUV3, located near the most northern head of Scripps Canyon, and PUV1 at the southern head of La Jolla Canyon (Fig 11-13). The focusing of energy at these two locations is consistent with the convergence of ray trajectories shown in Munk and Traylor's refraction diagram (Figure 14). Before reaching the canyons, swell has been refracted to the west by the continental shelf south of Pt. La Jolla. Additionally, waves are strongly refracted as they travel along the axis of each canyon. An extreme example of this process is seen in the directional spectrum of PUV1 (Figure 13), and PUV3 (Figure 11-12). Refraction over Scripps Canyon reverses the initial shift to the west, whereas at La Jolla Canyon, waves continue to turn to more northern arrival angles.

Swell energy decreases dramatically between the offshore wave buoy 100 and all other nearshore sensors. Much of this decay is caused by refraction over the Pt. La Jolla shelf. Additionally, rays are deflected by the two walls of each canyon, effectively creating a 'dead zone' at the head of the canyon. This is evident in the observed spectrum at buoy 115, which records about 2 orders of magnitude less energy than PUV3, and at buoy 116 where the swell peak has virtually disappeared (Figure 12). The extreme decay of energy at buoy 115 and 116 can be explained with the ray paths shown in Figure 14. Ray trajectories diverging away from Scripps Canyon carry very little energy, as these wave trains propagate from nearly the same offshore energy source.

Buoy 113 measures energy levels closest to the energy measured at buoy 100. At buoy 113's location, on the shelf north of Scripps Canyon, there is very little convergence or divergence. The mean direction of buoy 113 is more westerly than other nearshore buoys north of Scripps Canyon. Wave trains refracting across the continental shelf continue to refract westward as they turn to shore normal.

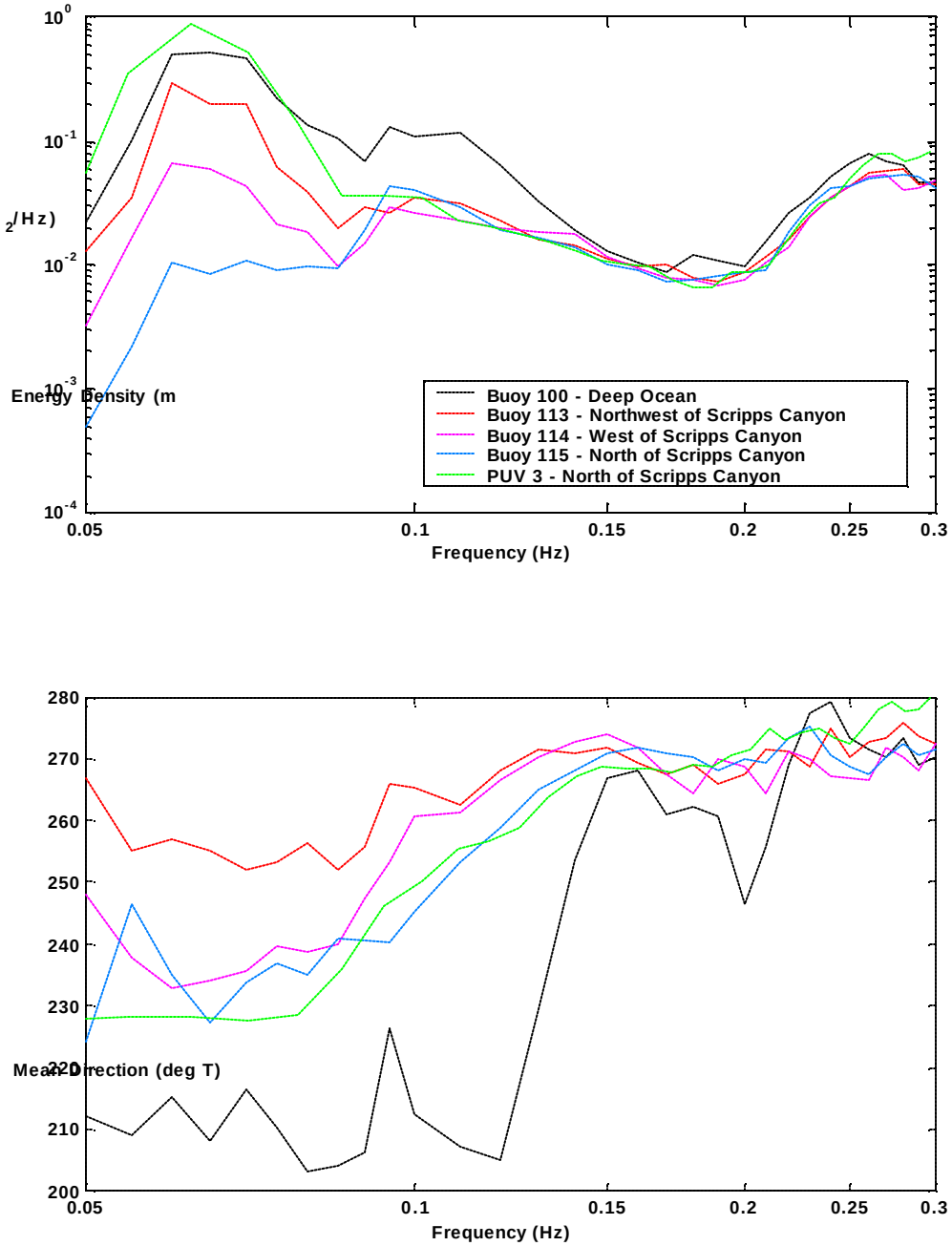

Figure 11. Observed energy density spectra and mean directions (as a function of frequency) north of Scripps Canyon on October 11th. The dashed lines indicate the incident wave conditions measured well offshore in deep water at the Outer Torrey Pines Buoy, buoy 100. Observations of wave conditions north of Scripps Canyon are indicated in color. Note the dramatic variations in wave conditions at swell (<0.1 Hz) frequencies.

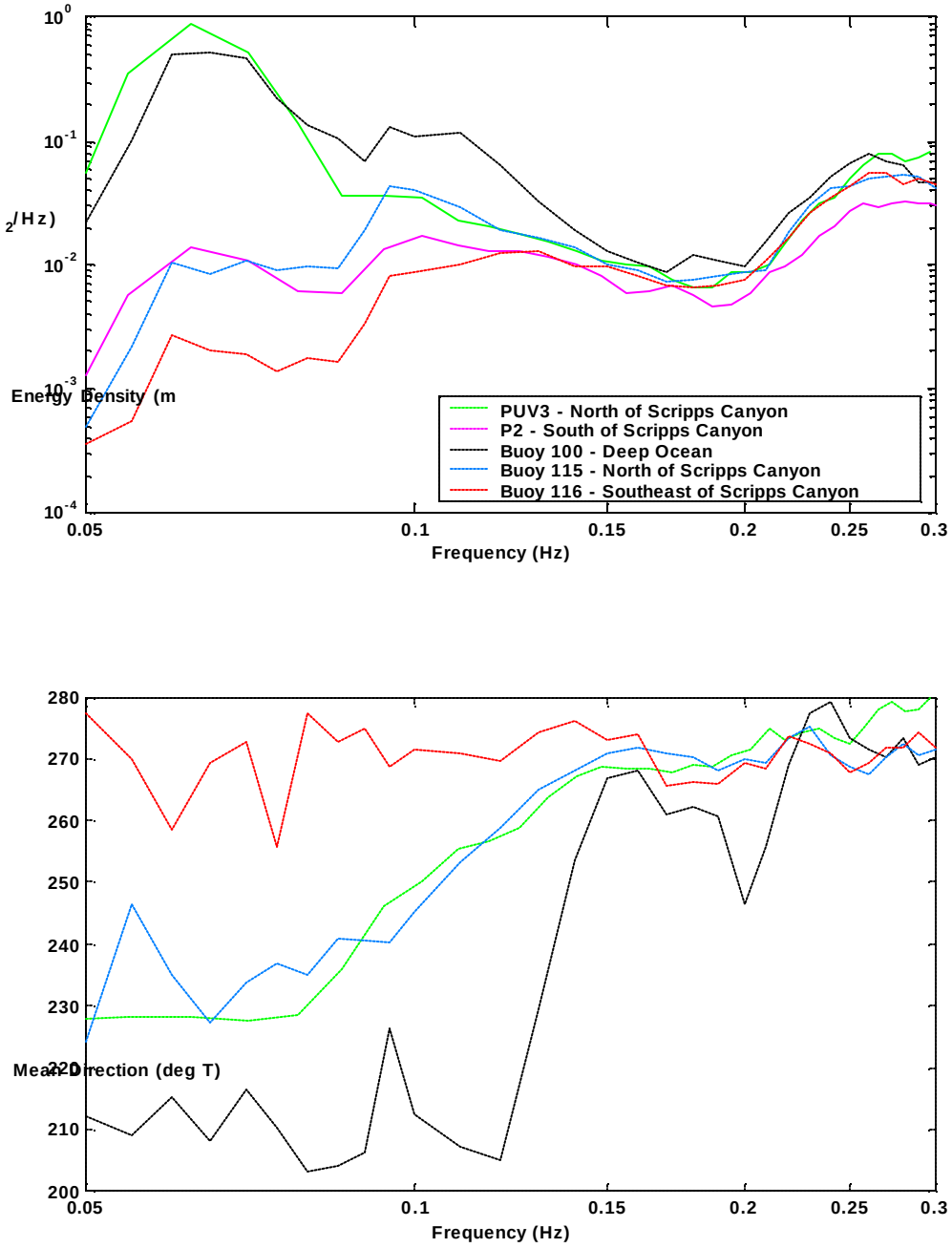

Figure 12. Observed energy density spectra and mean directions surrounding Scripps Canyon on October 11th. (same format as Figure 11)

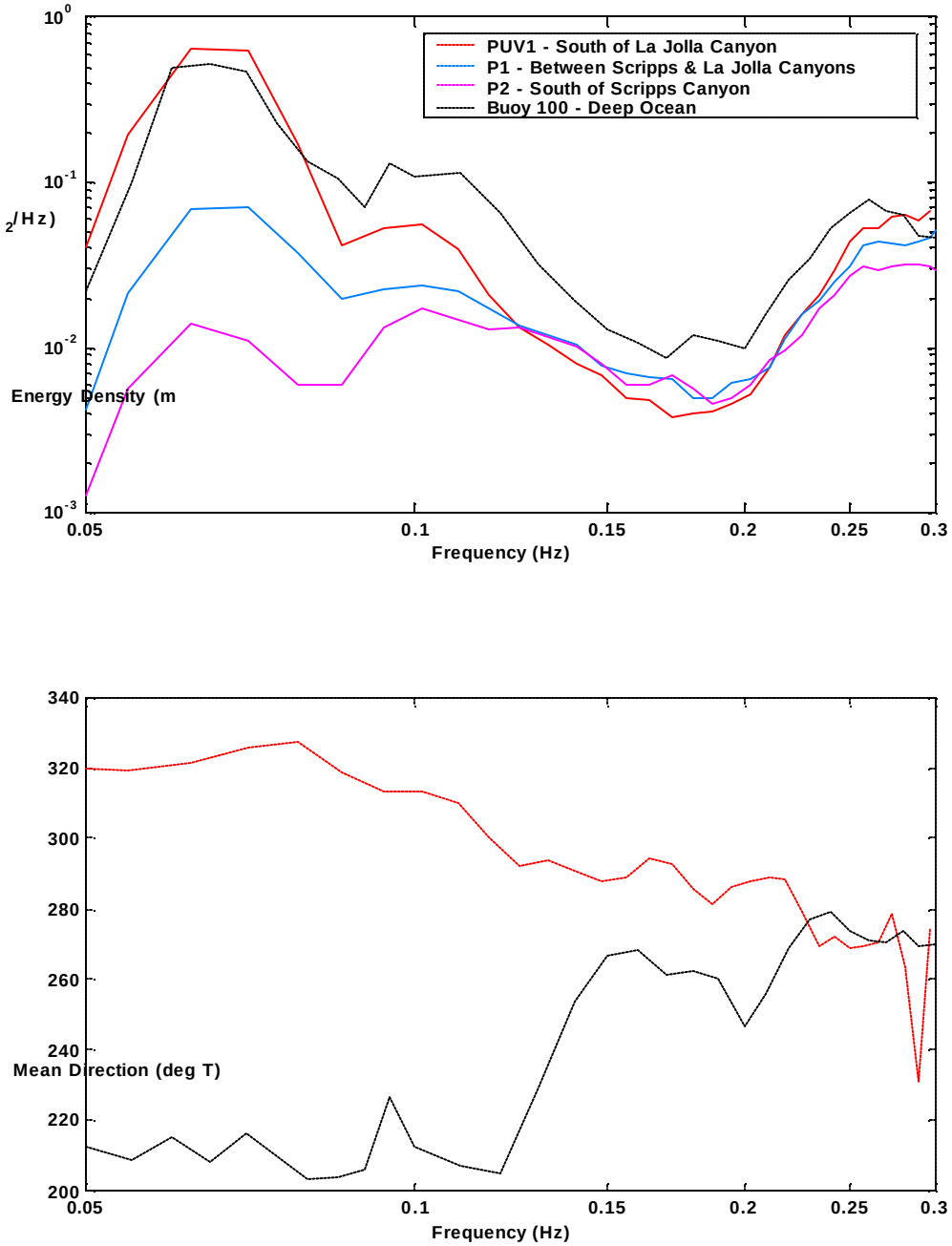

Figure 13. Observed energy density spectra and mean directions in the southern region of the canyon system on October 11th. P-sensor records do not contain directional information. Extreme refraction is evident in the observed turning of the mean direction at the swell peak by about 110º from 210º at buoy 100 to 320º at PUV1. (same format as Figure 11)

P2, located between the 'dead zone' east of Scripps Canyon and the convergence zone on the shelf between the canyons, records about the same level of energy as buoy 115. More energetic conditions in the convergence zone on the shelf between the canyons (Figure 14) are evident at P1 where the decay relative to the incident wave field is only 1 order of magnitude (Figure 13).

Energy variations are smaller at the secondary peak with a period of about 10.5 seconds. The decay of energy levels relative to incident energy is about a factor 3-10, and variations across the Scripps Canyon are considerably smaller than those observed at the primary swell peak.

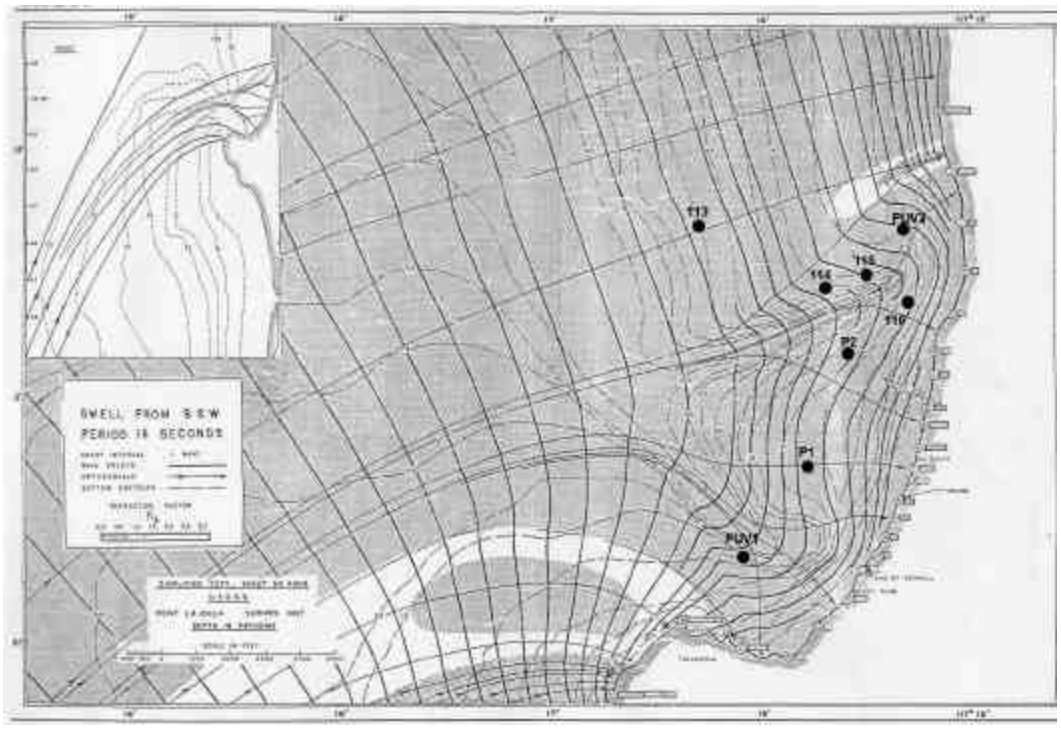

Figure 14. A refraction diagram for 16 second swell incident from the SSW -- conditions similar to those observed during the NCEX Pilot Experiment. (from Munk and Traylor, 1947)

There is very little evolution at wind wave frequencies (0.15 - 0.3 Hz), with differences in energy levels less than a factor 2 across the canyons, and differences in wave propagation direction less than 10º across the entire nearshore region. The relatively short wavelengths of these high frequency waves prevents interaction with the complex bathymetry of the canyon system, therefore reducing energy and directional

transformations. At the 0.25 Hz wind sea peak, waves are transformed by refraction only in depths less than about 10 meters, well inshore of the shallowest pressure sensor, P1, deployed in approximately 16 m depth.

B. 16 OCTOBER CASE STUDY

The October 16 case study shows qualitatively similar but considerably weaker variations in energy levels (Figure 15-17). Whereas swell energy levels measured on the northern side of Scripps Canyon varied by about 2 orders of magnitude on October 11 (Figure 11) they are within 0.85 orders of magnitude of each other on October 16 (Figure 15). Similarly, the amplification of energy levels at PUV3 (north of Scripps Canyon) and PUV1 (south of La Jolla Canyon) are less pronounced on October 16, as is the decay at buoy 116 located in the dead zone behind Scripps Canyon.

The changes in energy variation are most likely the result of the shifting of the incident swell direction to about 260º. As waves approach the canyon system from a more westerly direction, they experience less refraction at Scripps Canyon. Lower energy density at PUV3 may be due to reduced focusing at the head of Scripps Canyon. The change in the incident swell direction has exposed buoy 115 to more ocean swell, and as a result the wave field at buoy 115 has a factor 10 more energy than on October 11. No longer in the 'dead zone' caused by intense refraction at Scripps Canyon on October 11, buoy 116 now measures some swell energy that propagates across the canyon. Nevertheless, buoy 116 measures about 1 order of magnitude less energy than buoy 115, suggesting that the canyon is a strong barrier for these more westerly swell arrivals.

The energy amplification is also slightly weaker at PUV1 on October 16. With a mean direction of 320º that suggests that waves continue to experience considerable refraction at La Jolla Canyon. Similarly energy levels at P1 and P2 are less reduced compared to the open ocean swell energy (Figure 17).

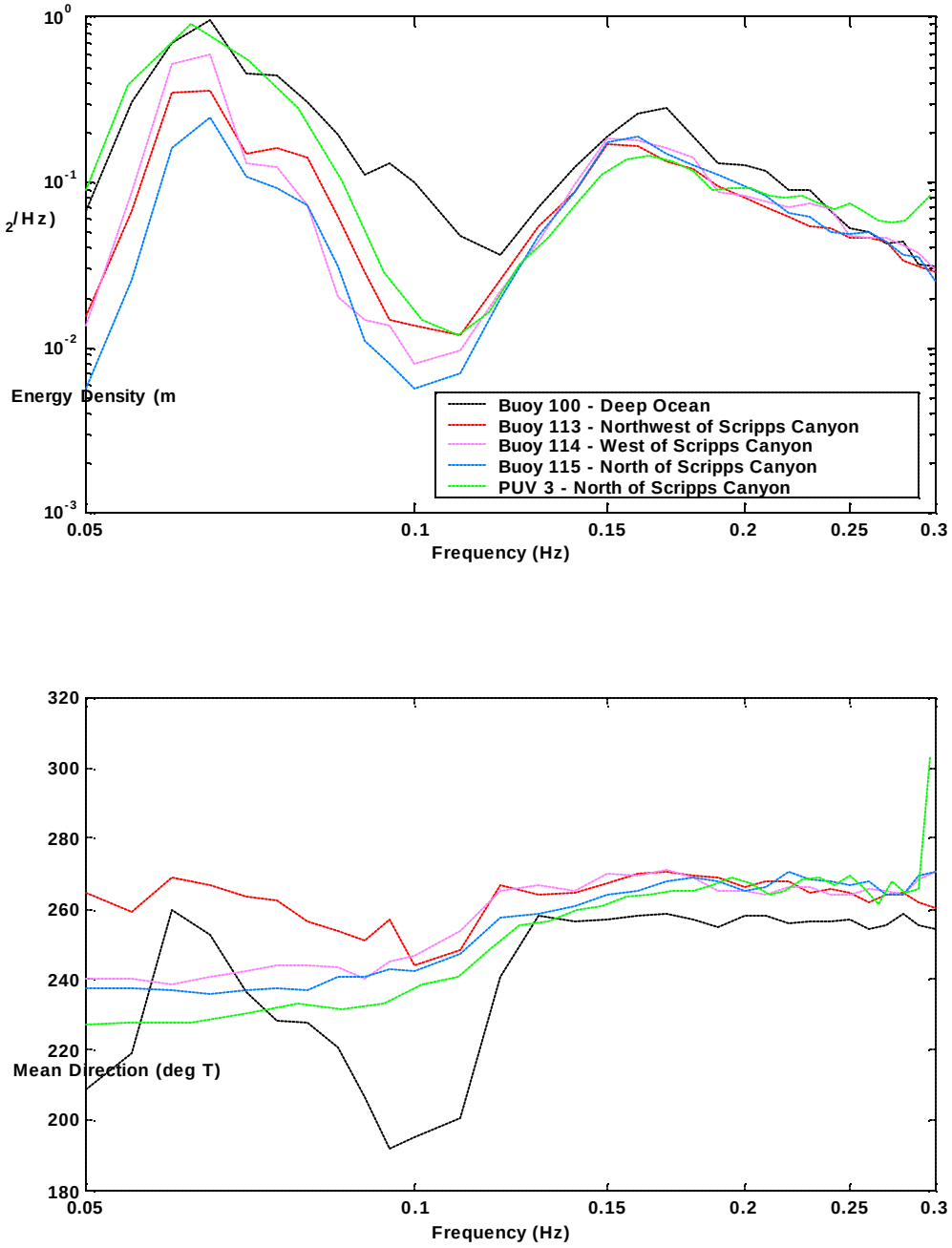

Figure 15. Energy and directional spectra at locations north of Scripps Canyon during the October 16th case study. (same format as Figure 11)

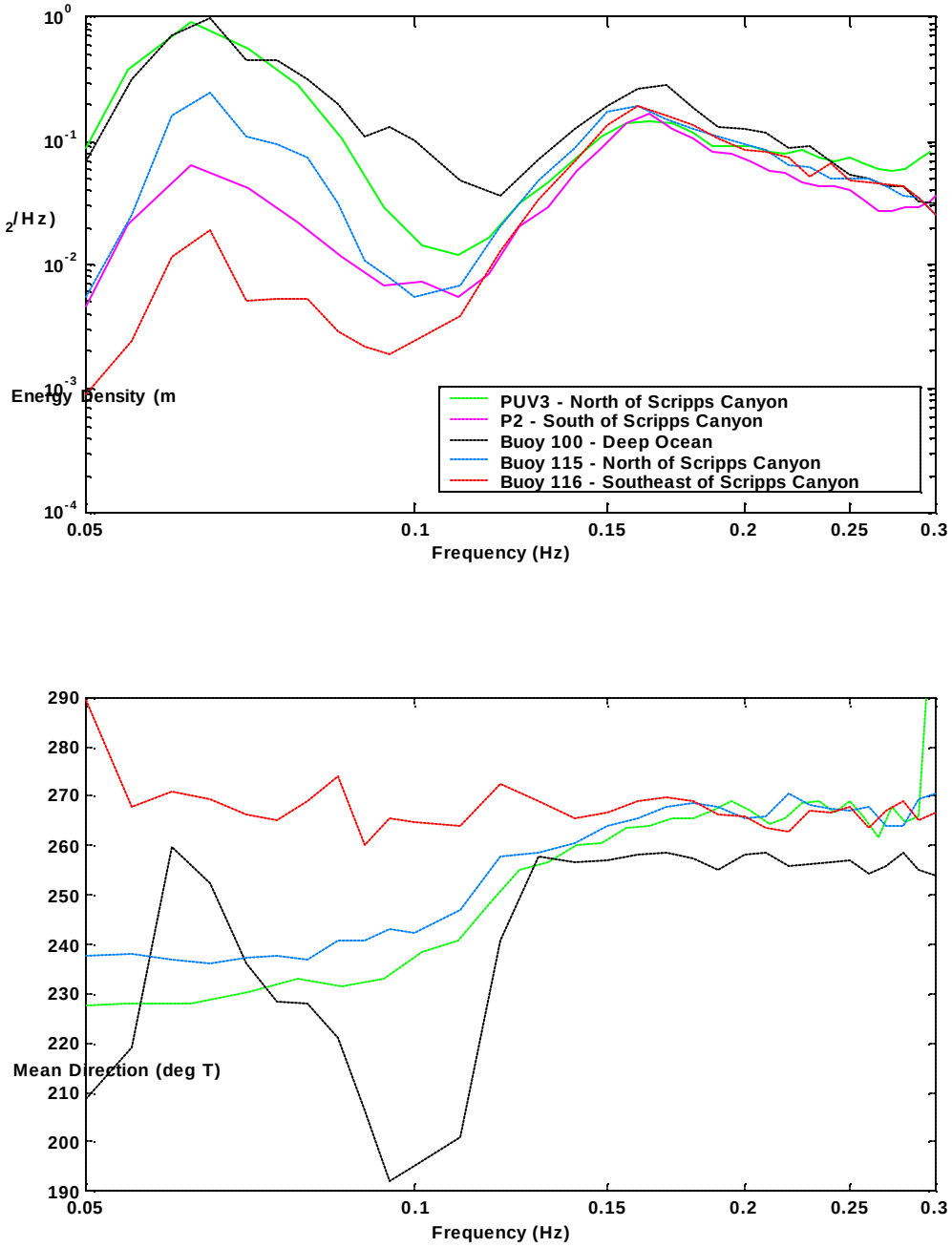

Figure 16. Energy and directional spectra at locations surrounding Scripps Canyon during the October 16th case study. (same format as Figure 11)

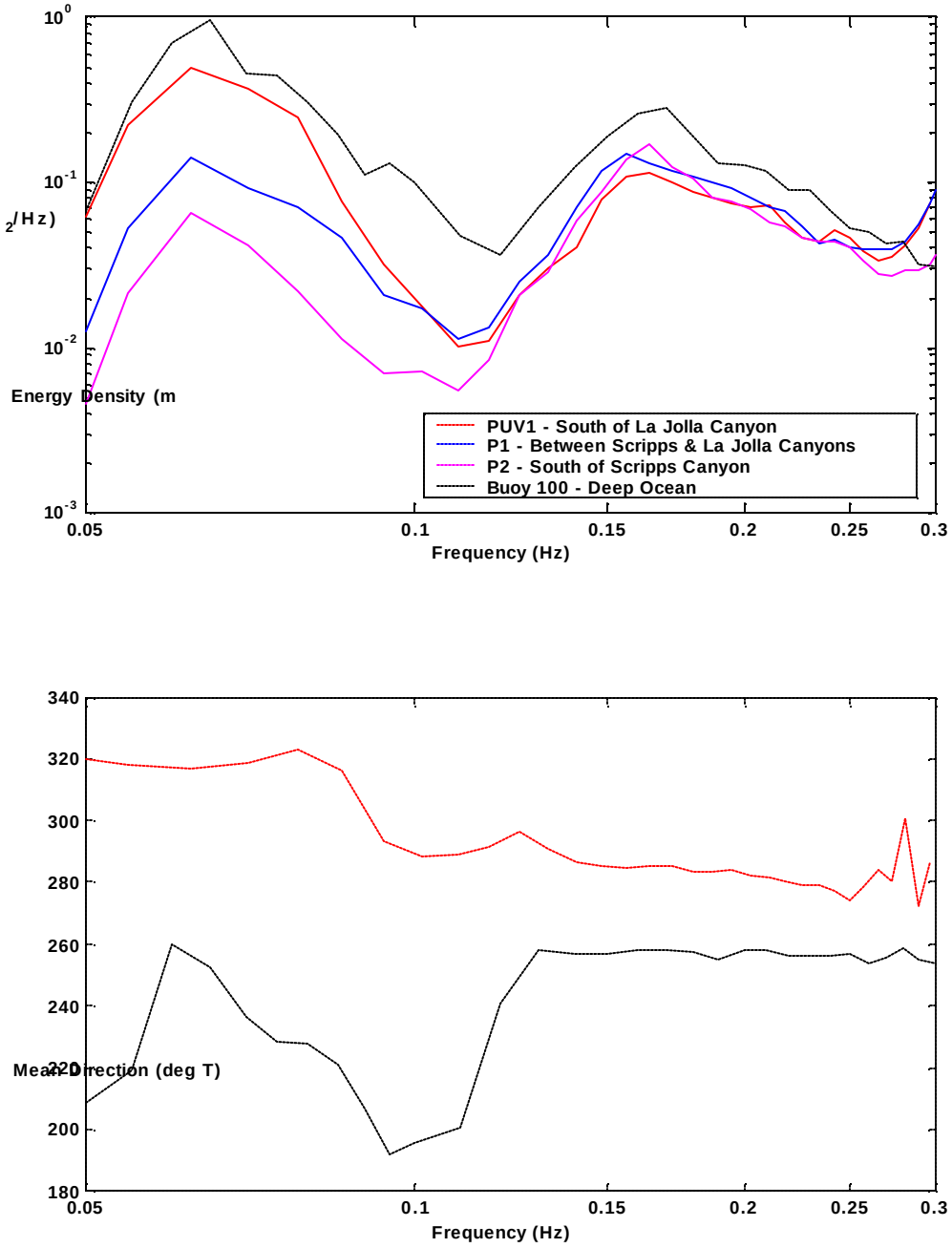

Figure 17. Energy and directional spectra at locations between Scripps Canyon and La Jolla Canyon, and south of La Jolla Canyon during the October 16th case study. (same format as Figure 11)

IV. COMPARISON OF OBSERVED AND PREDICTED SPECTRA

Accurate model predictions of wave energy and direction across the nearshore environment are increasingly valuable to naval strategists and tacticians planning nearshore naval operations. Existing operational models (e.g. WAM, WaveWatch, SWAN) can be configured to predict the effects of refraction, but often lack the resolution to resolve bathymetry in complex nearshore environments, adding considerable uncertainty to nearshore forecasts. Higher resolution models that are currently being assessed for use by the U.S. Navy require extensive verification with experimental groundtruths. In this chapter, the accuracy of a high-resolution linear back-refraction model is examined through comparisons with spectra collected by wavebuoys, PUVs, and pressure sensors deployed in the NCEX Pilot Experiment (described in the second and third chapters).

A. THE BACK-REFRACTION MODEL

The linear back-refraction model is based upon the assumption that wave energy is conserved along ray trajectories, neglecting energy sources or sinks. This approximation works well in small coastal regions where wave generation and dissipation often can be neglected and an accurate propagation scheme is needed to resolve the refraction of swell. Energy conservation is expressed as

$$S(f,\theta)) = \frac{k}{k_o}\frac{c_{go}}{c_g}\, S_o(f, \Gamma(f,\theta)) \qquad (1)$$

where S_0 is the incident wave spectrum obtained from measurements in deep water, S the predicted wave spectrum at a nearshore location, f is the frequency, k_0 and k are incident and local wave numbers, c_{g0} and c_g are incident and local group speeds, and Γ is the inverse direction function that can be obtained by back-refracting rays from the nearshore location to the open ocean. (see O'Reilly and Guza, 1991; and references therein) In order to accurately transform a spectrum from deep water to a nearshore instrument location, a large number of rays must be back-refracted to accurately define $\Gamma(f,\theta)$. Ray

paths are initially computed using the well-known geometrical optics relations from a selected nearshore location at 1º increments, then additional ray paths are added until rays reach the deep ocean at 1º increments, or the nearshore spacing falls below .01º (O'Reilly and Guza, 1992). The predicted energy levels at each nearshore location are calculated by applying Eq. 1 to the deep ocean incident spectra approximated by buoy 100. Although many rays are needed to adequately resolve the inverse direction function, Γ, over the complex bathymetry, these computations are performed only for the instrumented sites, and thus the back-refraction model is computationally efficient. (O'Reilly and Guza, 1991)

B. MODEL-DATA COMPARISONS

Spectra predicted by the back-refraction model are compared to the observed spectra analyzed in Chapter 3. In general, the model reproduces the observed energy variations well, and considering the complexity of the canyon bathymetry, the agreement is surprisingly good.

The model predictions accurately reproduce the extreme variations of energy density spectra and mean directions at swell frequencies observed on October 11 (Figure 18). The largest discrepancies are seen at sites with relatively low energy (e.g at buoy 115 and buoy 116). At high frequencies, where waves are not influenced by bottom topography, the predicted nearshore spectra are virtually unchanged from the incident offshore spectrum, in good agreement with observations.

On October 16, the predicted spectra confirm that the weaker variations of swell energy for westerly incidence angle (compared with the southerly swell arrival on October 11) are consistent with refraction predictions (compare Figure 18 and Figure 19). However, a large discrepancy between the predicted and observed spectra is noted at buoy 115. Here the predicted swell energy is almost an order of magnitude lower than the observed energy. Interestingly, the disagreement is seen only in the energy spectrum, whereas the observed and predicted mean directions agree well over the energetic band (0.06 - 0.13 Hz) of the spectrum.

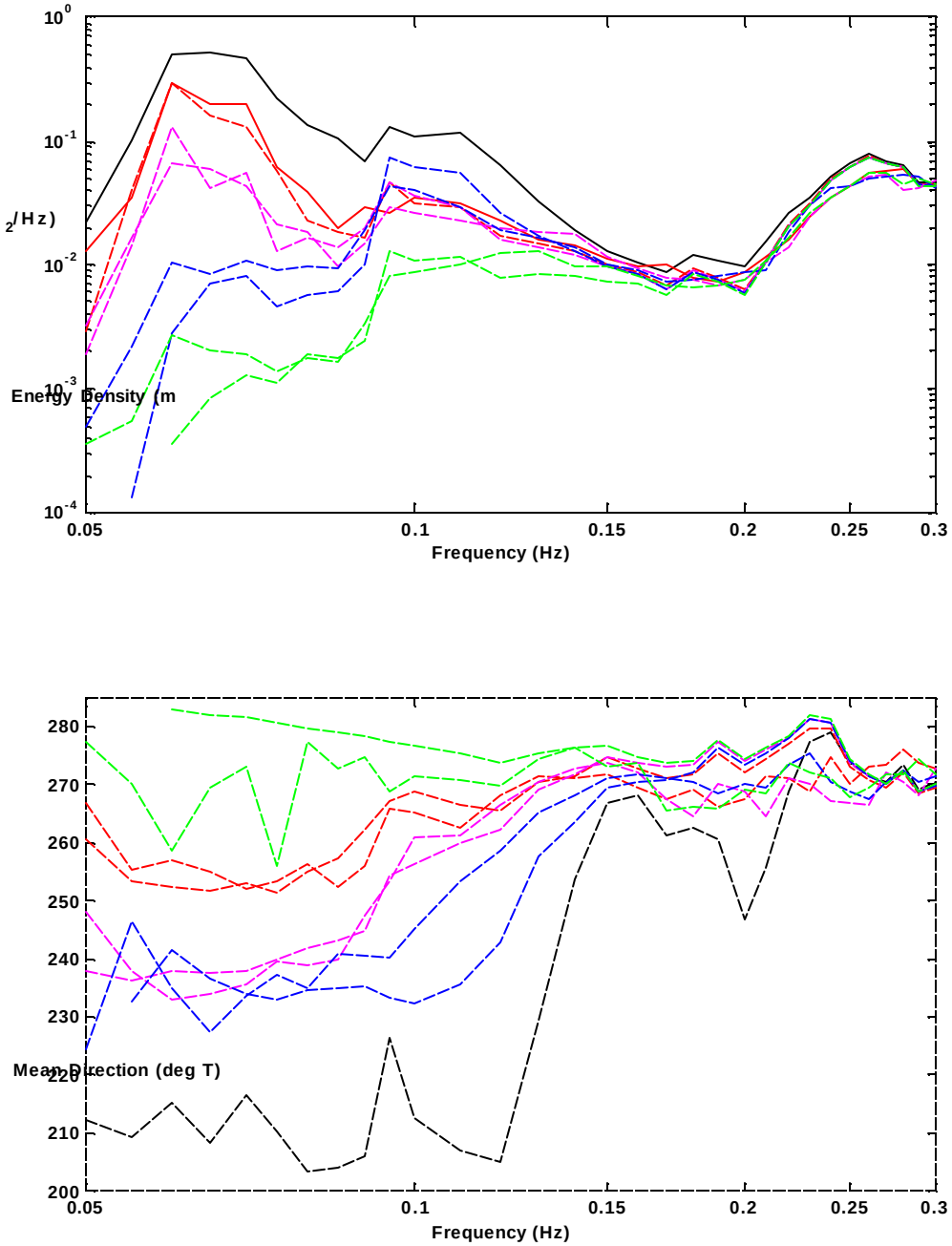

Figure 18 Observed (solid) and predicted (dashed) energy spectra and mean direction as a function of frequency on October 11. Buoy 100 provided the incident wave spectra for the back-refraction model calculation. Instrument locations are indicated with color: Buoy 100 - black, buoy 113 - red, buoy 114 - purple, buoy 115 - blue, and buoy 116 - green.

Buoy 115 is moored in 30 meters of water with about 60 meters of line near the north rim of Scripps Canyon. Energy levels at locations within the resulting watch-circle may be significantly different from the anchor location where the model prediction was evaluated. Buoy drift was considered as a possible cause of the large energy discrepancy at buoy 115. To investigate this hypothesis, the back-refraction model was run for locations 60 meters to the west and 60 meters to the north of the buoy 115 anchor location. These model predictions (Figure 20) indeed indicate strong model sensitivity at the steep wall of Scripps Canyon. The predicted spectrum 60 meters west of the presumed location of buoy 115 is in excellent agreement with the energy spectrum measured by buoy 115. However estimates of the drift of buoy 115 obtained from the GPS locations recorded at the buoy (Figure 21) show that the buoy was confined to an area southeast of the anchor site. Thus buoy-drift does not explain the model-data discrepancy.

A more plausible explanation of the discrepancy between observed and modeled spectra is an inaccuracy of the model prediction resulting from either the breakdown of refraction theory over steep bottom slopes or the limited spatial resolution of the model. The refraction model assumes a slowly varying smooth bathymetry, and thus predictions may be inaccurate near canyon walls. Model results are generally more accurate for locations with gentle bottom slopes, such as buoy 113. (Figures 18 and 19) By attempting to predict energy transformations on the side of Scripps Canyon, where the gradient is as steep as 7:1, we are obviously pushing the limits of the model. Furthermore, the refraction model has a grid resolution of about 0.0004 degrees (two grid cells in Figure 21) and may not accurately resolve the large wave energy gradients at the canyon wall.

Overall the agreement between the observations and refraction model predictions is remarkable considering the complexity and steepness of the bathymetry, and the results of this study suggest that a refraction model with adequate resolution can provide robust forecasts of wave conditions in this region.

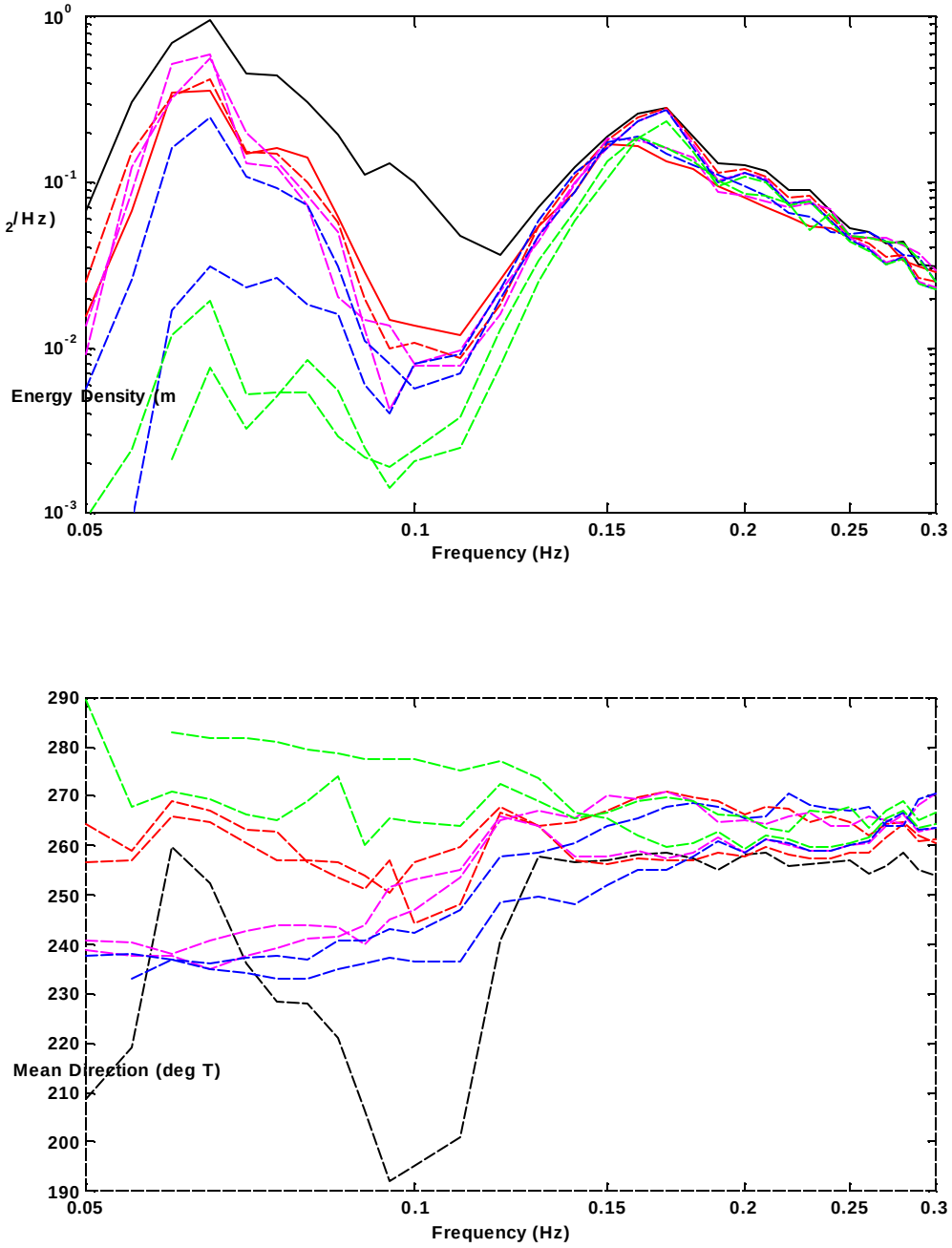

Figure 19. Observed (solid) and predicted (dashed) spectra on October 16. Buoy 100 provided the incident spectra for the back-refraction model calculation. Instrument locations are indicated with color: Buoy 100 - black, buoy 113 - red, buoy 114 - purple, buoy 115 - blue, and buoy 116 - green.

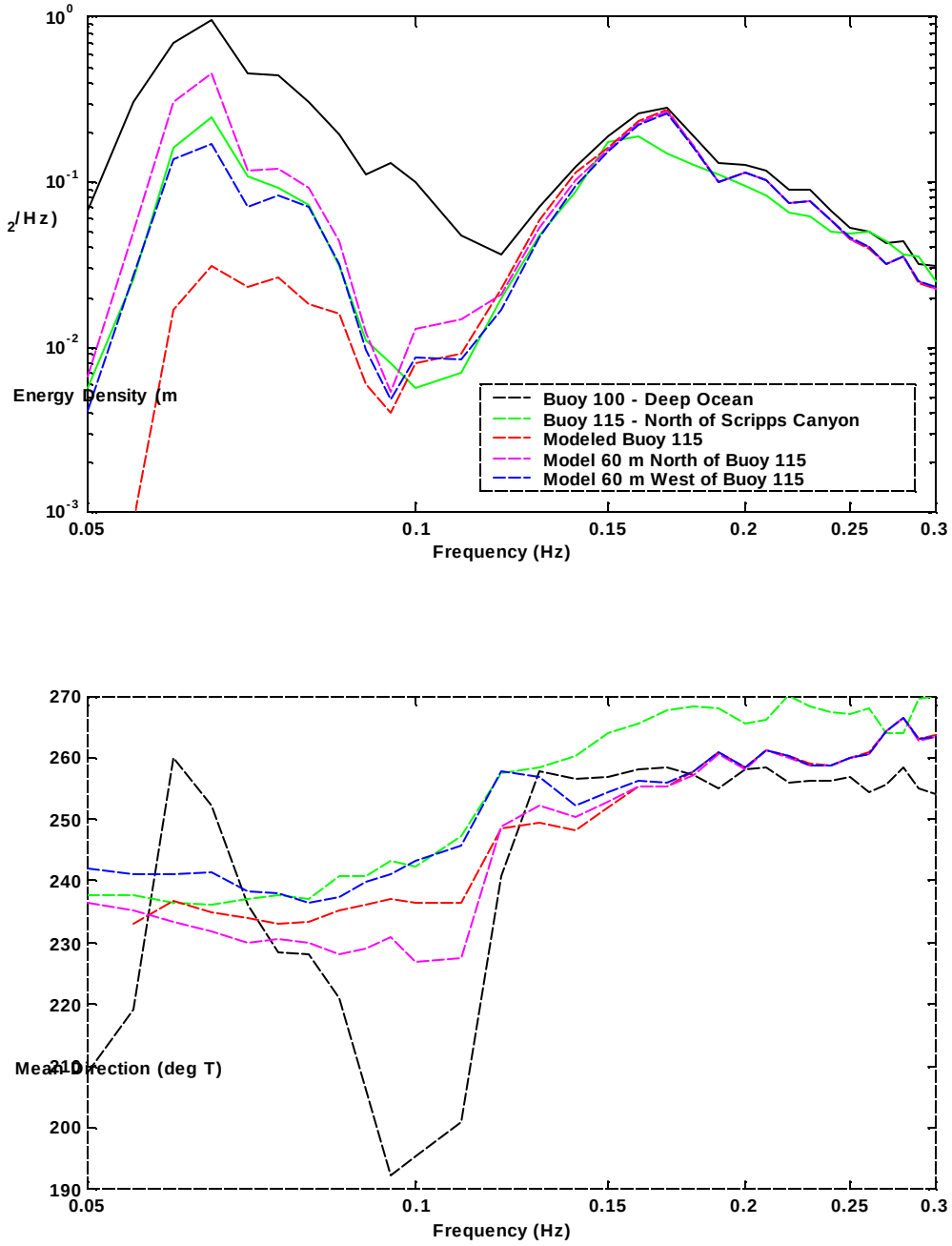

Figure 20. The spectra observed by buoy 100 and buoy 115, along with the modeled spectra at three locations: at buoy 115, 60 m north of buoy 115, and 60 m west of buoy 115. The modeled spectra 60 m north, and 60 m west of buoy 115 are in better agreement with the observed spectrum at buoy 115.

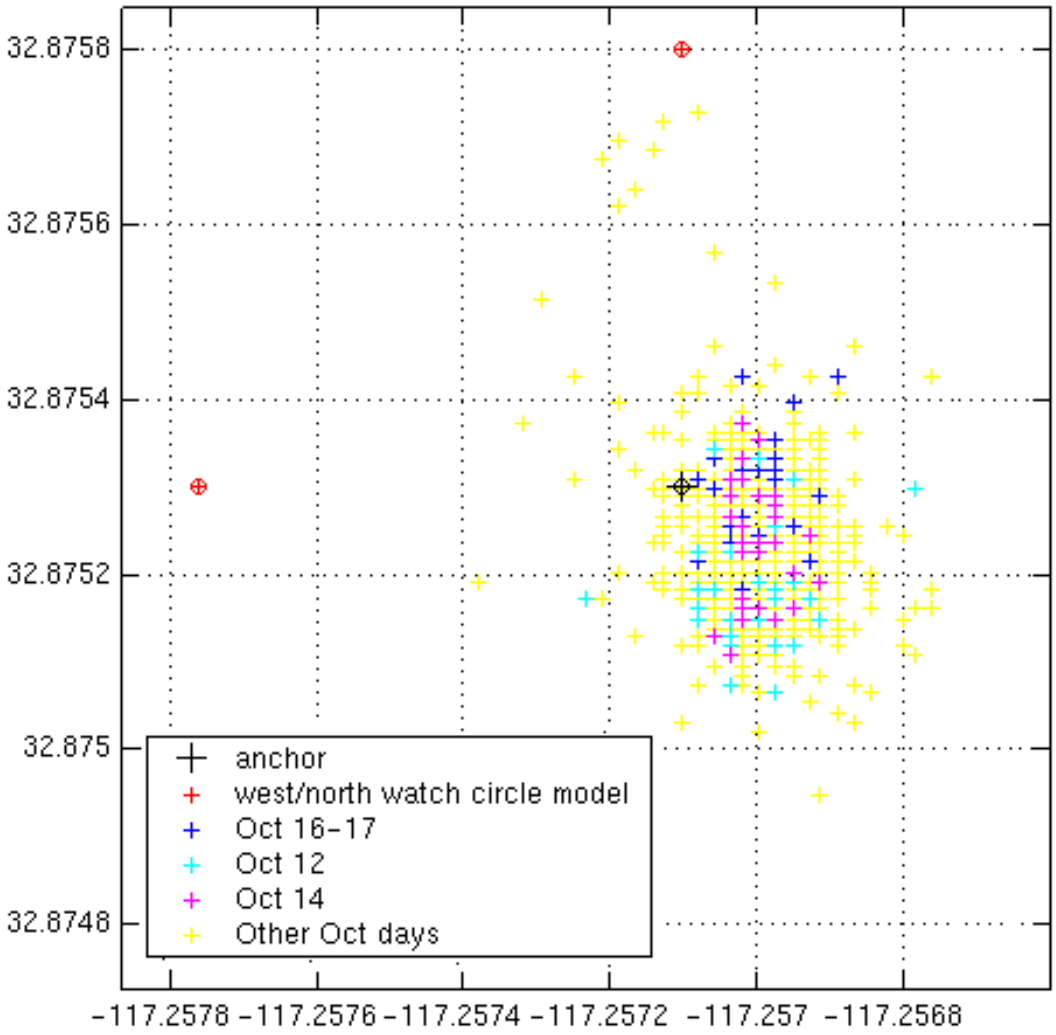

Figure 21. GPS tracked locations for buoy 115 over the course of the experiment. Although modeled spectra at locations 60 m west and north of the buoy (away from the canyon wall) were closer to observations made by buoy 115, the buoy drifted primarily to the southeast (into the canyon).

THIS PAGE INTENTIONALLY LEFT BLANK

V. SUMMARY AND CONCLUSIONS

Swell from distant storms propagates across thousands of kilometers of ocean in the form of straight and parallel long-crested wave fronts. As swell enters shallow water and interacts with bottom topography, refraction bends these wave fronts toward shallow depths,causing areas of energy convergence and divergence. In regions of complex bathymetry, such as offshore of Pt. La Jolla near San Diego, CA, refraction may cause extreme transformation of swell.

The Nearshore Canyon Experiment (NCEX) Pilot was designed as a preliminary study to quantify the effects of refraction caused by the complex bathymetry of the Scripps and La Jolla canyons. Four Datawell Directional Waverider Buoys, three Nortek Vector PUV Recorders, and two pressure sensors were deployed at locations of large expected energy transformation from 10 through 17 October 2002. The observations made during the NCEX Pilot show dramatic wave transformation over the submarine canyons, with refractive effects changing as a result of incident wave direction and local bathymetry. These observations are qualitatively consistent with observations and refraction diagrams produced by Munk and Traylor in their pioneering 1947 study of wave transformation over the same region.

Predictions of swell transformation, using a high-resolution spectral back-refraction model were compared to the NCEX Pilot observations. In general, predictions and observations are in good agreement. Large spatial variations of wave energy and direction are well captured by the model with some discrepancies in regions of unusually low wave energy and steep bottom slopes.

The observed wave transformation and the skill of the refraction model is summarized in Figure 22, showing observed and predicted significant wave heights (over the swell frequency range 0.03-0.10 Hz) at each sensor location in the Pt. La Jolla study region on October 11. Relatively large significant wave heights are observed and predicted at the focusing regions near the head of both canyons. In contrast, the significant wave height in the 'dead zone' to the east of Scripps Canyon is a factor 10 smaller than the wave height at the head of Scripps Canyon. Additionally, the back-

refraction predictions capture the less pronounced focusing of waves between the two canyons. Considering the complexity of the bathymetry across the entire nearshore region offshore of Pt. La Jolla, the results of the back-refraction model are of encouraging and confirm that refraction is the most significant factor in wave transformation in this region.

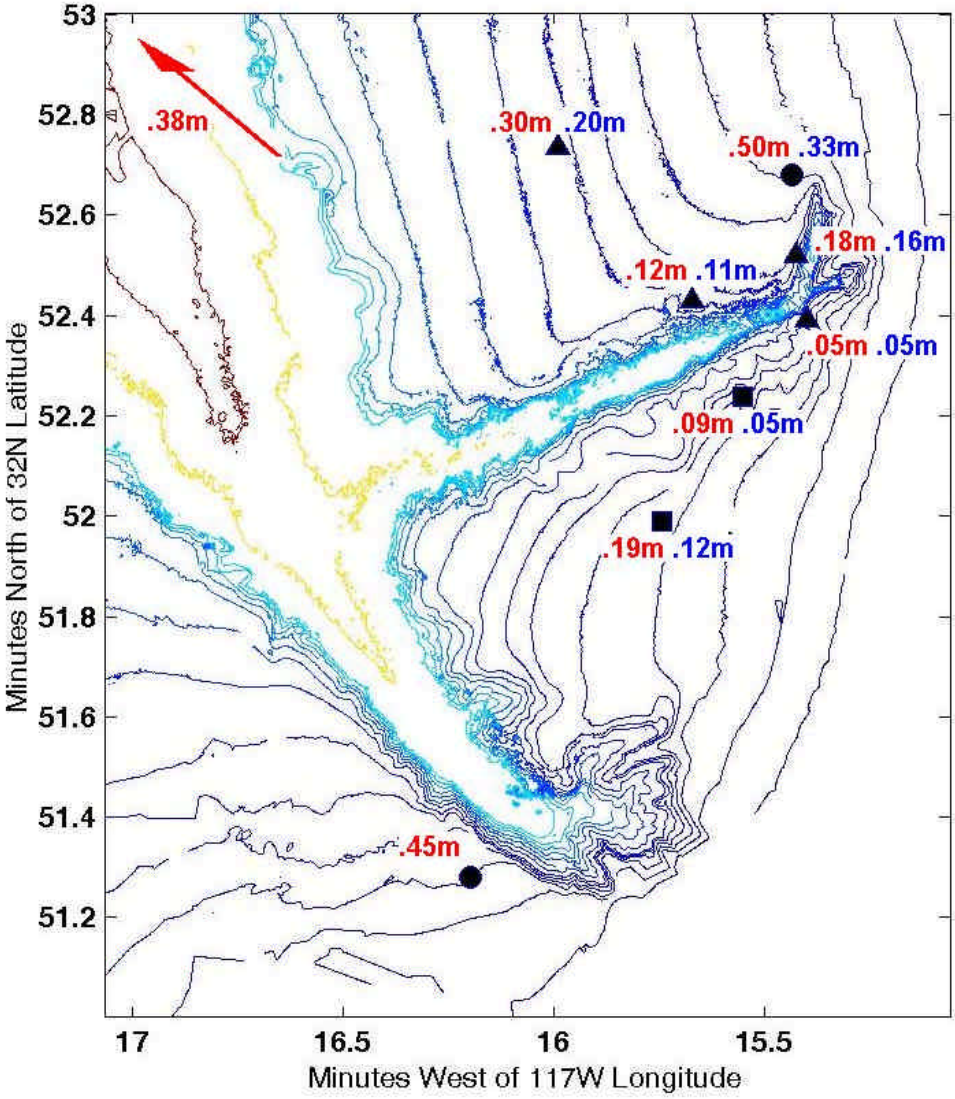

Figure 22. Observed and predicted significant wave height on October 11. Red and blue numbers correspond respectively to observed and predicted significant wave height. The incident significant wave height observed at buoy 100 was 0.38 m. Model predictions for PUV1 were not available, thus only the observed wave height is shown.

VI. LIST OF REFERENCES

Emery, K.O., 1958, Wave patterns off Southern California, Journal of Marine Research, vol.17, p.133-140.

Herbers, T.H.C., Elgar S., Guza, R.T., 1999, Directional spreading of waves in the nearshore, J. Geophys. Res., vol.104(C4), p.7683-7693.

Kirby, J.T., and Dalrymple, R.A., 1986, Modeling waves in surfzones and around islands, J Waterway. Port. Coastal Ocean Eng., vol.112, no.1, p.78-93.

Munk, W.H., and Traylor, M.A., 1947, Refraction of ocean waves: a process linking underwater topography to beach erosion, J. Geol., vol.55, no.1, p.1-26.

Munk, W.H., Miller, G.R., Snodgrass, F.E., and Barber, N.F., 1963, Directional recording of swell from distant storms, Phil. Trans. Roy. Soc. Lon., A255, p.506-584

O'Reilly, W.C., and Guza, R.T., 1991, Comparison of spectral refraction and refraction-diffraction wave model, J. Waterway. Port. Coastal Ocean Eng., vol.117. no.3 p.199-214.

O'Reilly, W.C., and Guza, R.T., 1992, A comparison of two spectral wave models in the Southern California Bight, Coastal Engineering, vol. 19, p.263-282.

Pawka, S.S., Inman, D.L., and Guza, R.T., 1984, Island sheltering of surface gravity waves: model and experiment, Continental Shelf Research, vol.3, no.1, p.35-53.

Shepard, F.P., and Inman, D.L., 1950, Nearshore water circulation related to bottom topography and wave refraction, Transactions, American Geophysical Union, vol.31, no.2, p.196-212.

Snodgrass, F.E., Groves, G.W., Hasselmann, K.F., Miller, G.R., Munk, W.H., and Powers, W.H., 1966, Propagation of ocean swell across the Pacific, Phil. Trans. Roy. Soc. Lon., vol.259, p.431-497.1.

THIS PAGE INTENTIONALLY LEFT BLANK

INITIAL DISTRIBUTION LIST

1. Defense Technical Information Center
   Ft. Belvoir, VA

2. Dudley Knox Library
   Naval Postgraduate School
   Monterey, CA

3. Professor T.H.C. Herbers, Code OC/He
   Department of Oceanography
   Naval Postgraduate School
   Monterey, CA

4. Professor M. L. Batteen
   Department of Oceanography
   Naval Postgraduate School
   Monterey, CA

5. Professor E.B. Thornton Code OC/Tm
   Department of Oceanography
   Naval Postgraduate School
   Monterey, CA

6. Mr. Paul Jessen
   Department of Oceanography
   Naval Postgraduate School
   Monterey, CA

7. Dr. W.C. O'Reilly
   Integrative Oceanography Division
   Scripps Institution of Oceanography
   La Jolla, CA

8. CAPT Dennis Whitford
   Department of Mathematics
   United States Naval Academy
   Annapolis, MD